Global fit of modified quark couplings to EW gauge bosons and vector-like quarks in light of the Cabibbo angle anomaly

Andreas Crivellin,[a,b] Matthew Kirk,[c] Teppei Kitahara[d,e,f] and Federico Mescia[c]

[a]*Physik-Institut, Universität Zürich, Winterthurerstrasse 190, 8057 Zürich, Switzerland*

[b]*Paul Scherrer Institut, 5232 Villigen PSI, Switzerland*

[c]*Departament de Física Quàntica i Astrofísica (FQA), Institut de Ciències del Cosmos (ICCUB), Universitat de Barcelona (UB), Barcelona, Spain*

[d]*IAR & KMI, Nagoya University, Nagoya 464-8602, Japan*

[e]*KEK Theory Center, IPNS, KEK, Tsukuba 305-0801, Japan*

[f]*CAS Key Laboratory of Theoretical Physics, ITP, CAS, Beijing 100190, China*

E-mail: andreas.crivellin@cern.ch, mjkirk@icc.ub.edu, teppeik@kmi.nagoya-u.ac.jp, mescia@ub.edu

Abstract: There are two tensions related to the Cabibbo angle of the CKM matrix. First, the determinations of V_{us} from $K_{\mu 2}$, $K_{\ell 3}$, and τ decays disagree at the 3σ level. Second, using the average of these results in combination with β decays (including super-allowed β decays and neutron decay), a deficit in first-row CKM unitarity with a significance of again about 3σ is found. These discrepancies, known as the Cabibbo Angle anomaly, can in principle be solved by modifications of W boson couplings to quarks. However, due to $\mathrm{SU}(2)_L$ invariance, Z couplings to quarks are also modified and flavour changing neutral currents can occur. In order to consistently assess the agreement of a new physics hypothesis with data, we perform a combined analysis for all dimension-six Standard Model Effective Field Theory operators that generate modified W couplings to first and second generation quarks. We then study models with vector-like quarks, which are prime candidates for a corresponding UV completion as they can affect W-quark couplings at tree level, and we perform a global fit including flavour observables (in particular loop effects in $\Delta F = 2$ processes). We find that the best fit can be obtained for the $\mathrm{SU}(2)_L$ doublet vector-like quark Q as it can generate right-handed W-u-d and W-u-s couplings as preferred by data.

Contents

1 Introduction

The Standard Model (SM) of particle physics has been very successfully tested and confirmed in the last decades with the Higgs discovery in 2012 providing the last missing constituent [1, 2]. As the Large Hadron Collider (LHC) at CERN has not (yet) found any new particles directly, precision experiments are becoming increasingly important to discover physics beyond the SM. In particular, an intriguing set of anomalies related to the violation of lepton flavour universality (see, e.g., refs. [3–6] for recent reviews) exist.

Among them, there is the so-called Cabibbo Angle Anomaly (CAA) [7–17] with a significance of currently around the 3σ level [18–20]. The CAA consists of two tensions related to the determination of the Cabibbo angle: first, the different determinations of $|V_{us}|$ from $K_{\mu 2}$, $K_{\ell 3}$, and τ decays disagree at the 3σ level. Second, using the average of these results in combination with β decays, a deficit in first-row Cabibbo-Kobayashi-Maskawa (CKM) unitarity appears with a significance at the 3σ level. While the deficit in the first-row unitarity could be related to lepton-flavour-universality violating new physics (NP), see refs. [21, 22] for reviews, such a setup cannot solve the tensions between the different

determinations of $|V_{us}|$. Intriguingly, however, both discrepancies (the CKM unitarity deficit and the tensions within $|V_{us}|$) could be explained via a modified W couplings to quarks.

Importantly, due to $\mathrm{SU}(2)_L$ invariance, such a modified W coupling to quarks in general leads to modified Z-quark-quark couplings as well, that enter electroweak precision observables, affect low-energy parity violation and can give contributions to the flavour changing neutral current (FCNC) processes. Therefore, a global fit is required to consistently assess the agreement of a specific NP scenario with data. The necessity of such a combined analysis becomes even more obvious when considering a UV complete model that can generate modified W couplings to quarks.

Here, we will study vector-like quarks (VLQs) as they give rise to such modifications already at tree level. While a new 4th generation of chiral fermions has been ruled out due to the combined constraints from LHC searches and flavour observables [23, 24], vector-like fermions can be added consistently without generating gauge anomalies. In fact, VLQs appear in many extensions of the SM such as grand unified theories [25–27], composite models or models with extra dimensions [28, 29] and little Higgs models [30, 31]. Furthermore, they have recently been studied intensively for phenomenological reasons since they can be considered part of the solution to $b \to s\ell^+\ell^-$ data [32–37], the tension in $(g-2)_\mu$ [38–55] and the W mass [56–59] and are prime candidates for explaining the CAA [7, 16, 60, 61]. In this case, not only the effect of modified Z couplings to quarks, like in the effective field theory (EFT) case, must be taken into account, but also loop effects in flavour observables have to be included in a global analysis.

In this paper we will perform such a global analysis, first for the Standard Model Effective Field Theory (SMEFT), and then for models with VLQs coupling to first and second generation quarks. We start by summarising the current status of the anomalies related to the Cabibbo angle in the next section. In section 3 we will describe the set up of our global fit, the matching of VLQs to the SMEFT, and discuss the relevant observables. Then in section 4.1 we use the global fit to analyse various EFT scenarios that correspond to modified gauge boson couplings to quarks, and see which scenarios provide the best fit to the current data. We then consider the different VLQ representations and their couplings to quarks in section 4.2 and conclude in section 5. Various useful results and further details are given in appendices A to D.

2 Current status of Cabibbo angle anomaly

In this section, we review the current situations of the $|V_{ud}|$ and $|V_{us}|$ determinations (which give rise to the CAA) summarized in figures 1–4 and table 1.

First, the CKM element $|V_{ud}|$ can be determined from various types of β decays. The latest determinations are $|V_{ud}|_{0^+ \to 0^+} = 0.97367(32)$ from the super-allowed $0^+ \to 0^+$ nuclear β decay [19, 63], $|V_{ud}|_{n(\mathrm{PDG})} = 0.97441(88)$ from the neutron decay [64], $|V_{ud}|_{\mathrm{mirror}} = 0.9739(10)$ from β transitions of the mirror nuclei [65], and $|V_{ud}|_{\pi_{e3}} = 0.9739(29)$ from the pion β decay ($\pi^+ \to \pi^0 e^+ \nu$; π_{e3}) [19, 66]. In these determinations, we use an estimation of ref. [19] for universal nuclear-independent radiative corrections from γW-box diagrams Δ_R^V [67] (see table 2). For the neutron decay, it is known that the uncertainty of $|V_{ud}|_{n(\mathrm{PDG})}$
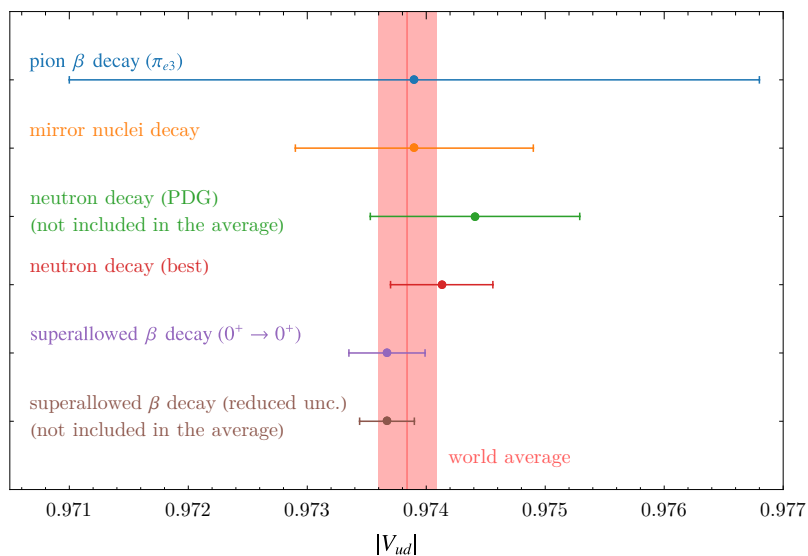
Figure 1. Summary of the determinations of $|V_{ud}|$ from the various types of β decays. The red band represents our world average (2.1). The details of the extractions from neutron decay (best) and the super-allowed β decays (reduced uncertainty) are given in the main text. Note that the pion β decay, even though it is currently not competitive, is theoretically clean and will be strikingly improved by the PIONEER experiment [62].
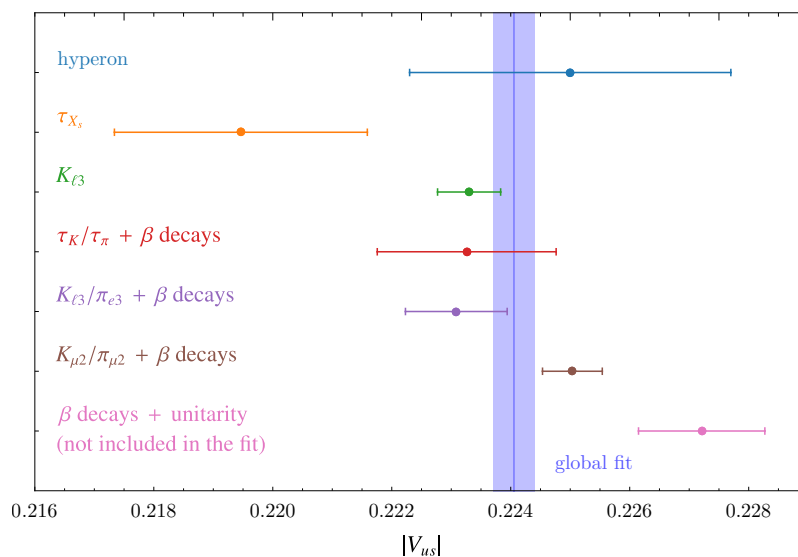

Figure 2. Summary of the determinations of $|V_{us}|$ from various processes. The global fit value of $|V_{us}|$ is obtained in eq. (2.11). Note that the global fit does not include the CKM unitarity constraint.

	Value	Observables	Label
V_{ud}	$0.973\,67 \pm 0.000\,32$	Q value and lifetime ft of super-allowed $0^+ \to 0^+$ nuclear β decays	$0^+ \to 0^+$
V_{ud}	$0.974\,13 \pm 0.000\,43$	τ_n [68] and g_A/g_V [69]	n (best)
V_{ud}	$0.974\,41 \pm 0.000\,88$	τ_n and g_A/g_V in PDG fit [64]	n (PDG)
V_{ud}	0.9739 ± 0.0010	ft of mirror nuclei decay	mirror
V_{ud}	0.9739 ± 0.0029	$\Gamma(\pi^+ \to \pi^0 e^+ \nu)$	π_{e3}
V_{ud}	$0.973\,84 \pm 0.000\,25$	world average w/o π_{e3} input	β
V_{ud}	$0.973\,84 \pm 0.000\,25$	world average	β
V_{us}	$0.223\,30 \pm 0.000\,53$	$\Gamma(K_{S,L} \to \pi^- \ell^+ \nu)$, $\Gamma(K^+ \to \pi^0 \ell^+ \nu)$	$K_{\ell 3}$
V_{us}	0.2195 ± 0.0021	$\Gamma(\tau \to X_s \nu)/\Gamma(\tau \to e \nu \bar\nu)$	τ_{X_s}
V_{us}	0.2250 ± 0.0027	$\Lambda^0 \to p, \Sigma^- \to n, \Xi^- \to \Lambda^0, \Xi^0 \to \Sigma^+$ semi-leptonic decays	hyperon
V_{us}	$0.223\,14 \pm 0.000\,51$	world average	K, τ, Λ
V_{us}/V_{ud}	$0.231\,08 \pm 0.000\,51$	$\Gamma(K^+ \to \mu^+ \nu)/\Gamma(\pi^+ \to \mu^+ \nu)$	$K_{\mu 2}/\pi_{\mu 2}$
V_{us}/V_{ud}	$0.229\,08 \pm 0.000\,88$	$\Gamma(K \to \pi \ell \nu)/\Gamma(\pi^+ \to \pi^0 e^+ \nu)$	$K_{\ell 3}/\pi_{e3}$
V_{us}/V_{ud}	0.2293 ± 0.0015	$\Gamma(\tau \to K^- \nu)/\Gamma(\tau \to \pi^- \nu)$	τ_K/τ_π
V_{us}/V_{ud}	$0.230\,47 \pm 0.000\,43$	world average	ratios
V_{ud}	$0.973\,79 \pm 0.000\,25$	global fit	global
V_{us}	$0.224\,05 \pm 0.000\,35$	global fit	global

Table 1. Up-to-date extractions of the CKM elements needed to test the first-row unitarity.

is inflated by scale factors which come from inconsistencies in the data. By using the single most precise result for the neutron lifetime τ_n [68] and the nucleon isovector axial charge g_A/g_V [69], a better determination of $|V_{ud}|_{n(\text{best})} = 0.97413(43)$ is possible [19]. Combining $|V_{ud}|_{0^+ \to 0^+}$, $|V_{ud}|_{n(\text{best})}$, $|V_{ud}|_{\text{mirror}}$, and $|V_{ud}|_{\pi_{e3}}$, we obtain a weighted average of

$$|V_{ud}|_\beta = 0.973\,84(25). \tag{2.1}$$

Here, any correlation among systematic uncertainties of the radiative corrections is discarded, which should be a good approximation because uncertainties of $|V_{ud}|$ are dominated by the experimental one except for the super-allowed β decays.[1]

Next, the matrix element $|V_{us}|$ can be determined from semi-leptonic decays of kaons and hyperons and from inclusive hadronic τ decays. By comparing theoretical predictions

---

[1]Note that the $|V_{ud}|$ determination is predominated by super-allowed β decays where the largest uncertainty comes from nuclear-structure (NS) dependent radiative corrections (corresponding to nuclear polarizability correction) [70], encoded in $\delta_{\text{NS},E}$ in ref. [63]. Unfortunately, precise estimations of $\delta_{\text{NS},E}$ are difficult [71] but the current value is considered to be very conservative [70]. Omitting the uncertainty from the $\delta_{\text{NS},E}$ corrections (see table 3), $|V_{ud}|_{0^+ \to 0^+(\text{reduced unc.})} = 0.97367(23)$ is obtained and the weighted average of the β decays becomes $|V_{ud}|_{\beta(\text{reduced unc.})} = 0.97378(20)$.

Parameter	Value	Source
$f_+^{K^0 \to \pi^-}(0)$	0.9698 ± 0.0017	FLAG 2021 $N_f = 2+1+1$ average, eq. (76) in [72]
$f_{K^\pm}/f_{\pi^\pm}$	1.1932 ± 0.0021	FLAG 2021 $N_f = 2+1+1$ average, eq. (81) in [72]
f_K/f_π	1.1978 ± 0.0022	Isospin-limit $N_f = 2+1+1$ average, Slide 34 of [73]
$\Delta_R^V (0^+ \to 0^+)$	$0.024\,67 \pm 0.000\,27$	Average of [9, 65, 74–77] from [19]
$\delta_{\mathrm{EM}}^{K^0 e} (K_{\ell 3})$	0.0116 ± 0.0003	Table VI in [78]
$\delta_{\mathrm{EM}}^{K^+ e} (K_{\ell 3})$	0.0021 ± 0.0005	Table VI in [78]
$\delta_{\mathrm{EM}}^{K^0 \mu} (K_{\ell 3})$	0.0154 ± 0.0004	Table IV in [79]
$\delta_{\mathrm{EM}}^{K^+ \mu} (K_{\ell 3})$	0.0005 ± 0.0005	Table IV in [79]
$\delta_{\mathrm{SU}(2)}^{K^+ \pi^0} (K_{\ell 3})$	0.0252 ± 0.0011	Given in [19] as $\Delta_{\mathrm{SU}(2)}$
$\delta_{\mathrm{EM}+\mathrm{SU}(2)}(K_{\mu 2}/\pi_{\mu 2})$	-0.0126 ± 0.0014	eq. (106) in [80]

Table 2. Updated values of the theoretical parameters which are used in this work. Δ_R^V is the universal nuclear-independent radiative correction to β decays (see main text for more details), δ_{EM} are the electromagnetic corrections to $K_{\ell 3}$ decays (see references for details), $\delta_{\mathrm{SU}(2)}$ is the isospin-breaking corrections to $K_{\ell 3}$ decays, and $\delta_{\mathrm{EM}+\mathrm{SU}(2)}$ is the difference in combined lattice calculations for electromagnetic and strong isospin-breaking corrections to $K_{\mu 2}$ and $\pi_{\mu 2}$.

with data of the semi-leptonic kaon decays $K_{S,L} \to \pi^- \ell^+ \nu$ and $K^+ \to \pi^0 \ell^+ \nu$ with $\ell = e, \mu$ (labelled $K_{\ell 3}$), one can obtain [19],

$$|V_{us}|_{K_{\ell 3}} = 0.223\,30(53)\,, \tag{2.2}$$

where the latest evaluations of the long-distance electromagnetic (EM) correction [78, 79, 81, 82], the strong isospin-breaking correction [19] (see table 2), and the recent K_S data from the KLOE-2 collaboration [83, 84] are used. Here, we also used the FLAG 2021 $N_f = 2 + 1 + 1$ value for $f_+^{K^0 \to \pi^-}(0)$,[2] and the form-factor parameters from ref. [73], see tables 2 and 3. Beyond kaons, one can also use the hyperon semi-leptonic decays, $(\Lambda \to p, \Sigma \to n, \Xi \to \Lambda, \Xi \to \Sigma)\,\ell\,\overline{\nu}$, which however lead to a slightly different yet less precise value [64, 87, 88]

$$|V_{us}|_{\mathrm{hyperon}} = 0.2250(27)\,. \tag{2.3}$$

Inclusive hadronic τ decays also provide an opportunity to extract the matrix element $|V_{us}|$ by separating the strange and non-strange hadronic states. Two representative determinations are reported: $|V_{us}|_{\mathrm{HFLAV}} = 0.2184(21)$ [89–91] and $|V_{us}|_{\mathrm{OPE+lattice}} = 0.2212(23)$ [92, 93]. The former is based on the conventional operator product expansion (OPE) with using the vacuum saturation approximation [94], while the later is based on

---

[2]Lattice works contributing to the $f_+^{K^0 \to \pi^-}(0)$ FLAG average are in refs. [85, 86].

Parameter	Value	Source
$\overline{\mathcal{F}t}\,(0^+ \to 0^+)$	$(3072.24 \pm 1.85)\,\mathrm{s}$	eq. (22) in Hardy and Towner [63]
	$(3072.24 \pm 1.21)\,\mathrm{s}$	Hardy and Towner [63] without uncertainty of $\delta_{\mathrm{NS},E}$, eq. (21) in [70]
$\Lambda_+\,(K_{\ell 3})$	$(25.55 \pm 0.38) \times 10^{-3}$	Slide 21 of [73]
$\ln C\,(K_{\ell 3})$	0.1992 ± 0.0078	Slide 21 of [73]

Table 3. Updated experimental inputs for the CKM determinations used in this work.

improved OPE series by fitting the lattice result [95].[3] Although they almost agree, there is no common consensus on which value, $|V_{us}|_{\mathrm{HFLAV}}$ or $|V_{us}|_{\mathrm{lattice}}$, to use [97]. Accordingly, we perform a weighted average of the two values

$$|V_{us}|_{\tau_{X_s}} = 0.2195(21)\,. \tag{2.4}$$

Here, a 100% correlation of the statistical uncertainty and a naive average of systematics uncertainty are taken into account for simplicity because they are based on the same data. By using these $|V_{us}|$ determinations, we obtain a weighted average of $|V_{us}|_{K_{\ell 3}}$, $|V_{us}|_{\mathrm{hyperon}}$, and $|V_{us}|_{\tau_{X_s}}$,

$$|V_{us}|_{K,\tau,\Lambda} = 0.223\,14(51)\,. \tag{2.5}$$

These $|V_{us}|$ values are summarized in figure 2 and table 1.

Third, the ratio $|V_{us}/V_{ud}|$ can be extracted from the several ratios of leptonic decay rates of kaon, pion and τ leptons. The leptonic kaon-decay rate over the pion one, $K_{\mu 2}/\pi_{\mu 2} = \Gamma(K^+ \to \mu^+\nu)/\Gamma(\pi^+ \to \mu^+\nu)$ provides [73]

$$\left|\frac{V_{us}}{V_{ud}}\right|_{K_{\mu 2}/\pi_{\mu 2}} = 0.231\,08(51)\,, \tag{2.6}$$

where the latest evaluation of the long-distance EM and strong isospin-breaking corrections [80, 98] is used, see table 2. Furthermore, the exclusive τ-decay ratio $\Gamma(\tau \to K^-\nu)/\Gamma(\tau \to \pi^-\nu)$ (labelled by τ_K/τ_π) provides [99] (see also refs. [100, 101])

$$\left|\frac{V_{us}}{V_{ud}}\right|_{\tau_K/\tau_\pi} = 0.2293(15)\,. \tag{2.7}$$

---

[3]Instead of the OPE approach, $|V_{us}|$ from the inclusive hadronic τ decays can be obtained based on the lattice-QCD simulation, where the spectral functions are evaluated by the lattice data of the hadronic vacuum polarization functions [72, 93, 96]. This lattice-based determination provides $|V_{us}|_{\mathrm{lattice}} = 0.2240(18)$. Although this $|V_{us}|_{\mathrm{lattice}}$ is a little more accurate compared to the others, it does mostly rely on the $\tau \to K^-\nu$ data [96], which is only $\sim 20\%$ of the inclusive strange-hadronic decays [90]. These facts imply that this determination does not well represent the sum of the exclusive τ decays, as well as an unknown correlation with $|V_{us}/V_{ud}|$ from exclusive τ decay (τ_K/τ_π in table 1). Therefore, we do not include this value in our analysis.

In both cases, to avoid the double counting of strong isospin-breaking contribution, we have made use of the isospin-limit $N_f = 2 + 1 + 1$ average for f_K/f_π, taken from ref. [73], see table 2.[4]

In addition, it is recently pointed out in ref. [102] that the semi-leptonic kaon-decay rate over the pion β decay, $\Gamma(K \to \pi\ell\nu)/\Gamma(\pi^+ \to \pi^0 e^+\nu)$ (labelled by $K_{\ell 3}/\pi_{e3}$), provides [82]

$$\left|\frac{V_{us}}{V_{ud}}\right|_{K_{\ell 3}/\pi_{e3}} = 0.229\,08(88)\,, \tag{2.8}$$

where the FLAG 2021 $N_f = 2 + 1 + 1$ average for $f_+^{K^0 \to \pi^-}(0)$ is used. Again, we obtain a weighted average of $|V_{us}/V_{ud}|_{K_{\mu 2}/\pi_{\mu 2}}$, $|V_{us}/V_{ud}|_{\tau_K/\tau_\pi}$ and $|V_{us}/V_{ud}|_{K_{\ell 3}/\pi_{e3}}$,

$$\left|\frac{V_{us}}{V_{ud}}\right|_{\text{ratios}} = 0.230\,47(43)\,. \tag{2.9}$$

Here, a correlation via the form factor f_K/f_π should be negligible because the uncertainty of $|V_{us}/V_{ud}|_{\tau_K/\tau_\pi}$ is dominated by the experimental data.

Finally, we perform a global analysis within the SM. In figures 3 and 4, the global fit result including $|V_{ud}|_\beta$, $|V_{us}|_{K,\tau,\Lambda}$ and $|V_{us}/V_{ud}|_{\text{ratios}}$ is shown by the blue circles. In figure 3, only β decays, $K_{\ell 3}$, $K_{\mu 2}/\pi_{\mu 2}$ and $K_{\ell 3}/\pi_{e3}$ are displayed (but all data are included in the global fit), while figure 4 shows all data. The black line stands for the unitarity condition: $|V_{ud}|^2 + |V_{us}|^2 + |V_{ub}|^2 = 1$ with $|V_{ub}| \approx 0.00377$ (from [103], one could also use [104], however the actual value is irrelevant due to its smallness). The blue shaded circle corresponds to $\Delta\chi^2 \leq 1$, while the dashed circle is $\Delta\chi^2 = 2.3$. In the χ^2 analysis, we included a correlation between $K_{\ell 3}$ and $K_{\ell 3}/\pi_{e3}$ because they share the same kaon data and common form factor $f_+^{K^0 \to \pi^-}(0)$. We set 100% correlation for these common uncertainties.

Our global fit results are

$$|V_{ud}|_{\text{global}} = 0.973\,79(25)\,, \tag{2.10}$$

$$|V_{us}|_{\text{global}} = 0.224\,05(35)\,, \tag{2.11}$$

and

$$\Delta_{\text{CKM}}^{\text{global}} \equiv |V_{ud}|_{\text{global}}^2 + |V_{us}|_{\text{global}}^2 + |V_{ub}|^2 - 1 = -0.001\,51(53)\,, \tag{2.12}$$

with a $|V_{ud}|_{\text{global}}$–$|V_{us}|_{\text{global}}$ correlation of 0.09. This $\Delta_{\text{CKM}}^{\text{global}}$ implies -2.8σ deviation from the unitarity condition of the CKM matrix.[5]

Also, one can define different CKM unitarity tests by taking each pair of the best measurements (β and the kaon decays) individually [19], which could distinguish each NP

---

[4]The decay constant from the FLAG 2021 [72], $f_{K^\pm}/f_{\pi^\pm} = 1.1932(21)$, contains the strong isospin-breaking contribution in the average.

[5]If one ignores the large uncertainty from the nuclear-structure dependent corrections to the super-allowed β decays and use $|V_{ud}|_{\beta\,(\text{reduced unc.})}$ (see footnote 1), a -3.7σ deviation from unitarity is observed in the global fit.
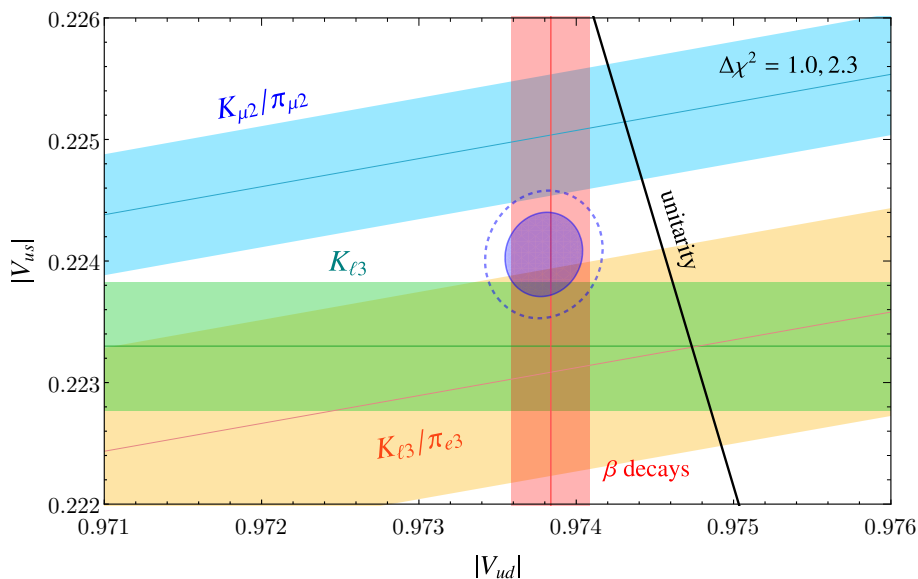
Figure 3. Global fit of all the available CKM determinations with $\Delta\chi^2 = 1$ (blue shaded) and $\Delta\chi^2 = 2.3$ (dashed circle). Only the 1σ regions from β decays, $K_{\ell 3}$, $K_{\mu 2}/\pi_{\mu 2}$ and $K_{\ell 3}/\pi_{e3}$ observables are shown. The black line represents the unitarity condition.
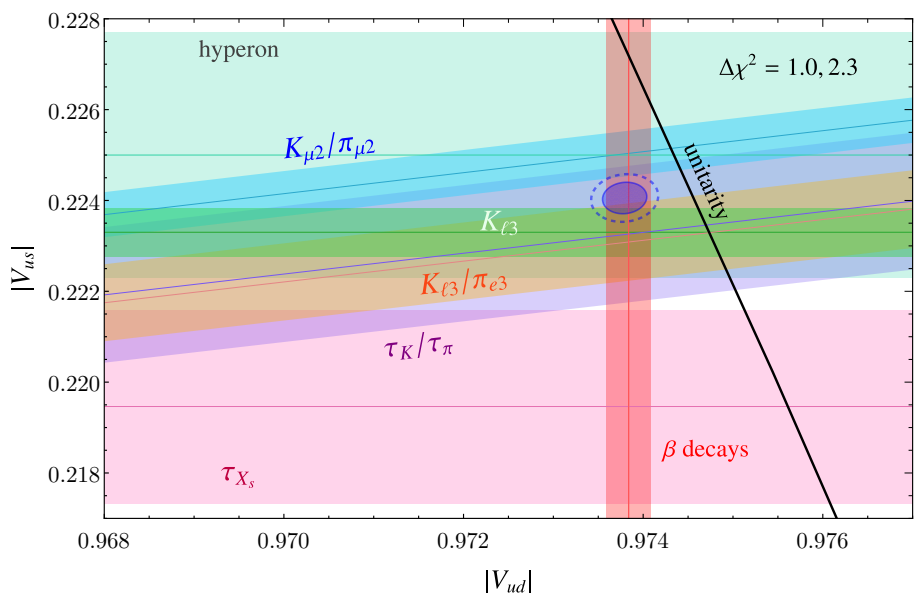

Figure 4. Same as figure 3, but the 1σ regions of $|V_{us}|_{\text{hyperon}}$, $|V_{us}|_{\tau_{X_s}}$ and $|V_{us}/V_{ud}|_{\tau_K/\tau_\pi}$ observables are also shown.

scenario,

$$\Delta_{\text{CKM}}^{(1)} \equiv |V_{ud}|_\beta^2 + |V_{us}|_{K_{\ell 3}}^2 + |V_{ub}|^2 - 1 \qquad\qquad = -0.001\,76(54)\,,$$

$$\Delta_{\text{CKM}}^{(2)} \equiv |V_{ud}|_\beta^2 + |V_{us}|_{K_{\mu 2}/\pi_{\mu 2},\,\beta}^2 + |V_{ub}|^2 - 1 \qquad = -0.000\,98(56)\,, \qquad (2.13)$$

$$\Delta_{\text{CKM}}^{(3)} \equiv |V_{ud}|_{K_{\mu 2}/\pi_{\mu 2},\,K_{\ell 3}}^2 + |V_{us}|_{K_{\ell 3}}^2 + |V_{ub}|^2 - 1 \quad = -0.0163(62)\,,$$

corresponding to -3.3σ, -1.8σ, -2.6σ discrepancies, respectively.

We summarize the determinations of $|V_{us}|$ from various observables in figure 2. There, the blue band represents the global fit of $|V_{us}|$ in eq. (2.11) in which the CKM unitarity condition is not included. It is shown that $|V_{us}|_{\tau_{X_s}}$ (orange bar) is a little bit smaller than the other determinations; 3.3σ, 2.6σ, 1.8σ discrepancies by comparing to β decays with unitarity (magenta), $K_{\mu 2}/\pi_{\mu 2}$ with β decays (brown), and $K_{\ell 3}$ (green), respectively.

Before closing this section, we give a brief summary of the status of *first-column* CKM unitarity, i.e., $|V_{ud}|^2 + |V_{cd}|^2 + |V_{td}|^2 = 1$. The CKM element $|V_{cd}|$ can be determined from leptonic and semi-leptonic D-meson decays and by a charmed-hadron production via neutrino-nucleon scattering [105]. The world average is $|V_{cd}| = 0.221(4)$ [64], which is dominated by $D^+ \to \mu^+\nu$ [106]. The element $|V_{td}|$ can be determined indirectly by global CKM fit. The current world average is $|V_{td}| = 0.0086(2)$ [64], however, the actual value is irrelevant due to its smallness. Combining this in a global fit with $|V_{ud}|$ of eq. (2.10), we find the first-column CKM unitarity

$$\Delta_{\text{CKM}}^{1^{\text{st}}\text{column}} \equiv |V_{ud}|_{\text{global}}^2 + |V_{cd}|^2 + |V_{td}|^2 - 1 = -0.0028(18)\,, \qquad (2.14)$$

implying deviation of 1.5σ. Here, the statistical uncertainty of $D^+ \to \mu^+\nu$ [90] dominates, which will be reduced by the Belle II [107] and BES III experiments [108].

3 Setup

In this section we first establish our conventions for the SMEFT and the extensions of the SM by VLQs. We then discuss our fit method and the most important constraints used in the global analysis.

3.1 SMEFT

We write the SMEFT Lagrangian as

$$\mathcal{L}_{\text{SMEFT}} = \mathcal{L}_{\text{SM}} + \sum_i C_i Q_i\,, \qquad (3.1)$$

such that the SMEFT coefficients have dimensions of inverse mass squared. We use the Warsaw basis [109], as well as the corresponding conventions, in which the operators generating modified gauge-boson couplings to quarks (at tree-level) are given by

$$Q_{Hq}^{(1)ij} = (H^\dagger i \overset{\leftrightarrow}{D}_\mu H)(\bar{q}_i \gamma^\mu P_L q_j)\,, \qquad\qquad Q_{Hq}^{(3)ij} = (H^\dagger i \overset{\leftrightarrow}{D}_\mu^I H)(\bar{q}_i \tau^I \gamma^\mu P_L q_j)\,,$$

$$Q_{Hu}^{ij} = (H^\dagger i \overset{\leftrightarrow}{D}_\mu H)(\bar{u}_i \gamma^\mu P_R u_j)\,, \qquad\qquad Q_{Hd}^{ij} = (H^\dagger i \overset{\leftrightarrow}{D}_\mu H)(\bar{d}_i \gamma^\mu P_R d_j)\,,$$

$$Q_{Hud}^{ij} = i(\tilde{H}^\dagger D_\mu H)(\bar{u}_i \gamma^\mu P_R d_j)\,. \qquad\qquad (3.2)$$

We work in the down-basis such that CKM elements appear in transitions involving left-handed up-type quarks after electroweak (EW) symmetry breaking. This means we write the left-handed quarks doublet as $q_i^T = \left((V^\dagger u_L)_i \; d_{L,i} \right)$, where V is the CKM matrix. With this conventions, the modified W and Z couplings are given by

$$
\begin{aligned}
\mathcal{L}_{W,Z} = & -\frac{g_2}{\sqrt{2}} W_\mu^+ \, \bar{u}_i \gamma^\mu \left(\left[V \cdot \left(\mathbb{1} + v^2 C_{Hq}^{(3)} \right) \right]_{ij} P_L + \frac{v^2}{2} \left[C_{Hud} \right]_{ij} P_R \right) d_j + \text{h.c.} \qquad (3.3) \\
& -\frac{g_2}{6 c_W} Z_\mu \, \bar{u}_i \gamma^\mu \left(\left[(3 - 4 s_W^2) \mathbb{1} + 3 v^2 \, V \cdot \left\{ C_{Hq}^{(3)} - C_{Hq}^{(1)} \right\} \cdot V^\dagger \right]_{ij} P_L \right. \\
& \hspace{4cm} \left. - \left[4 s_W^2 \mathbb{1} + 3 v^2 C_{Hu} \right]_{ij} P_R \right) u_j \\
& -\frac{g_2}{6 c_W} Z_\mu \, \bar{d}_i \gamma^\mu \left(\left[(2 s_W^2 - 3) \mathbb{1} + 3 v^2 \left\{ C_{Hq}^{(3)} + C_{Hq}^{(1)} \right\} \right]_{ij} P_L \right. \\
& \hspace{4cm} \left. + \left[2 s_W^2 \mathbb{1} + 3 v^2 C_{Hd} \right]_{ij} P_R \right) d_j \,,
\end{aligned}
$$

where $v \approx 246\,\text{GeV}$.

3.2 Vector-like quarks

There are seven possible VLQs that can mix with SM quarks after EW symmetry breaking:

$$
\begin{aligned}
& U : (\mathbf{3}, \mathbf{1}, {}^2\!/_3)\,, \qquad D : (\mathbf{3}, \mathbf{1}, -{}^1\!/_3)\,, \quad Q : (\mathbf{3}, \mathbf{2}, {}^1\!/_6)\,, \\
& Q_5 : (\mathbf{3}, \mathbf{2}, -{}^5\!/_6)\,, \quad Q_7 : (\mathbf{3}, \mathbf{2}, {}^7\!/_6)\,, \qquad\qquad\qquad\qquad (3.4)\\
& T_1 : (\mathbf{3}, \mathbf{3}, -{}^1\!/_3)\,, \quad T_2 : (\mathbf{3}, \mathbf{3}, {}^2\!/_3)\,.
\end{aligned}
$$

The numbers in the brackets denote the representation under the SM gauge group $\mathrm{SU}(3) \times \mathrm{SU}(2)_L \times \mathrm{U}(1)_Y$. The Lagrangian describing their interactions with the Higgs and SM quarks is

$$
\begin{aligned}
-\mathcal{L}_{\text{VLQ}} = & \; \xi_{fi}^U \bar{U}_f \tilde{H}^\dagger q_i + \xi_{fi}^D \bar{D}_f H^\dagger q_i + \xi_{fi}^u \bar{Q}_f \tilde{H} u_i + \xi_{fi}^d \bar{Q}_f H d_i \qquad\qquad (3.5) \\
& + \xi_{fi}^{Q_5} \bar{Q}_{5,f} \tilde{H} d_i + \xi_{fi}^{Q_7} \bar{Q}_{7,f} H u_i + \frac{1}{2} \xi_{fi}^{T_1} H^\dagger \tau \cdot \bar{T}_{1,f} q_i + \frac{1}{2} \xi_{fi}^{T_2} \tilde{H}^\dagger \tau \cdot \bar{T}_{2,f} q_i + \text{h.c.} \,,
\end{aligned}
$$

where q is the left-handed quark doublet, u, d are the right handed quark singlets, and i and f are flavour indices for the SM quarks and new VLQs, respectively. Note that therefore f does not necessarily need to run from 1 to 3 as the number of generations of VLQs is arbitrary (i.e. unknown). We disregard possible couplings between two VLQs representations and the SM Higgs as they are not relevant (at the dimension-six level) for the modification of gauge boson couplings to quarks.

With these conventions, the matching obtained by integrating out the VLQs at tree level onto the SMEFT is

$$[C_{Hu}]_{ij} = -\frac{\xi_{fj}^u \xi_{fi}^{u*}}{2M_{Q_f}^2} + \frac{\xi_{fj}^{Q_7} \xi_{fi}^{Q_7*}}{2M_{Q_{7f}}^2},$$

$$[C_{Hd}]_{ij} = \frac{\xi_{fj}^d \xi_{fi}^{d*}}{2M_{Q_f}^2} - \frac{\xi_{fj}^{Q_5} \xi_{fi}^{Q_5*}}{2M_{Q_{5f}}^2},$$

$$[C_{Hud}]_{ij} = \frac{\xi_{fj}^d \xi_{fi}^{u*}}{M_{Q_f}^2}, \tag{3.6}$$

$$\left[C_{Hq}^{(1)}\right]_{ij} = \frac{\xi_{fj}^U \xi_{fi}^{U*}}{4M_{U_f}^2} - \frac{\xi_{fj}^D \xi_{fi}^{D*}}{4M_{D_f}^2} - \frac{3\xi_{fj}^{T_1} \xi_{fi}^{T_1*}}{16M_{T_{1f}}^2} + \frac{3\xi_{fj}^{T_2} \xi_{fi}^{T_2*}}{16M_{T_{2f}}^2},$$

$$\left[C_{Hq}^{(3)}\right]_{ij} = -\frac{\xi_{fj}^U \xi_{fi}^{U*}}{4M_{U_f}^2} - \frac{\xi_{fj}^D \xi_{fi}^{D*}}{4M_{D_f}^2} + \frac{\xi_{fj}^{T_1} \xi_{fi}^{T_1*}}{16M_{T_{1f}}^2} + \frac{\xi_{fj}^{T_2} \xi_{fi}^{T_2*}}{16M_{T_{2f}}^2}.$$

Note that C_{uH} and C_{dH} are also generated at tree-level, but as being proportional to the tiny masses of first and second generation quarks, they are not relevant for our study (if the couplings of the Higgs to two different VLQs are neglected). In Higgs decays, this suppression is removed when normalising to the SM rate, however these decays have not been measured (nor are they expected to be in the near future), and for flavour observables the quark mass suppression compared to the effects from the modified gauge boson couplings is restored. At one-loop, there are also contributions to the $\Delta F = 2$ operators $Q_{qq}^{(1,3)}$, $Q_{qu}^{(1,8)}$, and C_{uu} which affect D^0–$\bar{\mathrm{D}}^0$ and kaon mixing and give rise to relevant bounds. The full expressions for the related Wilson coefficients can be found in appendix A.[6]

3.3 Fit method and observables

We use `smelli v2.3.2` [112, 113] (which is built on `flavio` [114] for the observable calculations, and `wilson` [115] for the RG evolution in the SMEFT and the low-energy EFT (LEFT)) for our global fit. To efficiently sample the likelihood in our scenarios with more than two free parameters, we use an MCMC library `PyMultiNest` [116–118] with the software package `corner` [119] for visualisation.

Since our NP effects change the extraction of the CKM elements, the theory predictions of CKM dependent observables are non-trivial and a consistent treatment is necessary. Following ref. [120] we determine the Cabibbo angle, at each parameter point in parameters space using $K_{\mu 2}/\pi_{\mu 2}$ as input and take into account the NP effects, and then calculate V_{ud} and V_{us} using the unitarity of the CKM matrix of the SM Lagrangian.[7] This then fixes the

---

[6]At one-loop, the Wilson coefficient of SMEFT operator Q_{HD}, which modifies the W mass, is generated. The latest results from CDF II [110], which hint at a sizable deviation from the SM prediction, could be explained by VLQs with large couplings, i.e., bigger than one. However, we do not consider this possibility here and therefore do not include the measurement in the global fit. For the interested reader, a recent study of the W mass in VLQ models has been performed in ref. [111].

[7]Note that choosing $K_{\mu 2}/\pi_{\mu 2}$ to determine the Cabibbo angle is arbitrary in the sense that any other determination could be used and the final result of the global fit does not depend on this choice of the input scheme.

theory parameters necessary for the calculation of the other observables that depend on CKM elements which are then compared to their measured values when performing the fit.

In our fit we include all β decays, along with $K_{\ell 3}$. The two exclusive τ decays $\tau \to \pi\nu$ and $\tau \to K\nu$ are included separately, rather than as a single ratio. We also include charged-current D decays (since these are strongly sensitive to $V_{cd} \approx -V_{us}$), with both total branching ratios and individual q^2-binned data.[8] Furthermore, in the later figures we refer to a single "CKM" region, this means the region in which all the different charged-current observables (listed explicitly in tables 5 to 8 and eq. (2.4)) are in best agreement with data. Note also that this extraction of the CKM elements, is also used later in the calculation of the SM prediction for CP violation in kaon mixing (ϵ_K).

The most relevant observables already contained within `smelli`, which we updated with our input (see tables 2 and 3), are listed in appendix C. Concerning kaon FCNC observables, both $\Delta S = 2$ (ϵ_K) and $\Delta S = 1$ ($K \to \pi\nu\nu$ and $K \to \ell^+\ell^-$) are included. Specifically concerning ϵ_K, using our input parameters, `flavio` gives a SM prediction for ϵ_K of $(2.12 \pm 0.32) \times 10^{-3}$. Compared to the prediction in ref. [121], we have an 80 % larger error, which can be mainly attributed to larger CKM uncertainties due to our BSM CKM treatment described above. It has previously been shown in refs. [122–124] that the dominant NP contribution to ϵ_K comes through diagrams with a Z-s-d on one side, and a SM one-loop correction on the other, which leads to enhanced sensitivity to right-handed Z-s-d couplings. In our fit, these effects are taken into account through the one-loop matching of the SMEFT onto the LEFT, as implemented in `wilson`. Finally, for the effects in D^0–$\overline{\mathrm{D}}^0$ mixing, we include the one-loop induced $\Delta F = 2$ coefficients, along with contributions from two insertions of the $\Delta F = 1$ modified Z couplings, which are formally of dimension-eight in the SMEFT power counting. However, since a reliable SM prediction for ΔM_D is still unavailable, to be conservative (and also in light of our partial inclusion of dimension-eight SMEFT effects) we use a Gaussian likelihood for the NP contribution with mean 0 and standard deviation equal to the current experimental central value [90, 125].

In addition to these observables already present in `smelli`, we implemented low-energy parity violation in `flavio`, based on ref. [126], which can provide similarly strong bounds on VLQs as electroweak precision measurements. For this we added to the likelihood a contribution which comes from the Q_{weak} experiment [127] and the measurement of atomic parity violation in $^{133}\mathrm{Cs}$ [128–130]. We also include a contribution from inclusive τ decays, based on our combination detailed above.

4 Analysis and results

We now perform our global analysis with the method and observables discussed in the last section. We start with the SMEFT where we use the Wilson coefficients as input at a scale of 1 TeV and evolve them to the scale of the observables, while for the VLQs we consider a matching scale of 2 TeV.

---

[8]Note that we added these manually, since they are not included by default in `smelli` v2.3.2, but they will be included in a future public release of `smelli`.

4.1 SMEFT results for modified gauge boson couplings

First of all, according to eq. (3.3), while both $\left[C_{Hq}^{(3)}\right]_{11}$ (which generates a modification of the left-handed W-u-d coupling) and $[C_{Hud}]_{11}$ (which generates a right-handed W-u-d coupling) can in principle explain the deficit in first-row CKM unitarity, the disagreement between V_{us} from $K_{\mu2}$, $K_{\ell3}$ and τ decays can only be accounted for by $[C_{Hud}]_{12}$, i.e. a right-handed W-u-s coupling is necessary [131] (see appendix B for details). Therefore, we will focus on scenarios with these coefficients in the following.

1-D scenarios. First, we consider a non-zero value of the Wilson coefficient $\left[C_{Hq}^{(3)}\right]_{11}$, where from our global fit we find

$$\left[C_{Hq}^{(3)}\right]_{11} \times v^2 = (-0.50 \pm 0.25) \times 10^{-3}\,. \tag{4.1}$$

As we are working in the down-basis, no constraints from kaon physics arise, however, CKM rotations lead to effects in D^0–$\bar{D}^0$ mixing, which are (despite our very conservative bound and the fact that it is a dimension-eight effect) stronger than the electroweak precision observables (EWPO) (see top-left panel in figure 5). However, the bounds from D^0–$\bar{D}^0$ mixing can be weakened or avoided by using a flavour structure that respects U(2) flavour ($\left[C_{Hq}^{(3)}\right]_{11} = \left[C_{Hq}^{(3)}\right]_{22}$) or by cancelling the effect in Z couplings to up quarks via $\left[C_{Hq}^{(3)}\right]_{11} = \left[C_{Hq}^{(1)}\right]_{11}$, respectively. For these two scenarios, shown in the top-middle and top-right panel of figure 5, we find

$$\left[C_{Hq}^{(3)}\right]_{11} = \left[C_{Hq}^{(3)}\right]_{22} \times v^2 = (-0.27 \pm 0.25) \times 10^{-3}\,, \tag{4.2}$$

$$\left[C_{Hq}^{(3)}\right]_{11} = \left[C_{Hq}^{(1)}\right]_{11} \times v^2 = (-0.55 \pm 0.28) \times 10^{-3}\,. \tag{4.3}$$

Considering instead modifications of the right-handed W-u-d or W-u-s vertex, no effects in D^0–$\bar{D}^0$ mixing and Z-pole observables arise (see bottom panels in figure 5) and we find

$$[C_{Hud}]_{11} \times v^2 = (-1.0 \pm 0.6) \times 10^{-3}\,, \tag{4.4}$$

$$[C_{Hud}]_{12} \times v^2 = (-2.0 \pm 0.7) \times 10^{-3}\,, \tag{4.5}$$

The corresponding pulls for all scenarios are given in table 4.

2-D scenarios. As we have seen in the previous paragraph, non-zero values of $[C_{Hud}]_{11}$ and $[C_{Hud}]_{12}$ lead to modifications of right-handed W-u-d and W-u-s couplings and are able to solve and alleviate the tensions within V_{us} and the unitarity deficit, respectively. The resulting preferred regions in the corresponding plane are shown in the left panel of figure 6. Note that while inclusive τ decays are not directly sensitive to right-handed currents, we get a constraint here since they modify the extraction of V_{us} (in our scheme), leading to an indirect sensitivity. On the other hand, despite exclusive τ decays being more precise, they do not present a constraint here as their theoretical prediction is affected in the same way as $K_{\mu2}/\pi_{\mu2}$ used as an input in our scheme.

Alternatively we can consider non-zero values of $\left[C_{Hq}^{(3)}\right]_{11}$ and $[C_{Hud}]_{12}$ if we aim at explaining both tensions, leading to modifications of the left-handed W-u-d and a right-handed
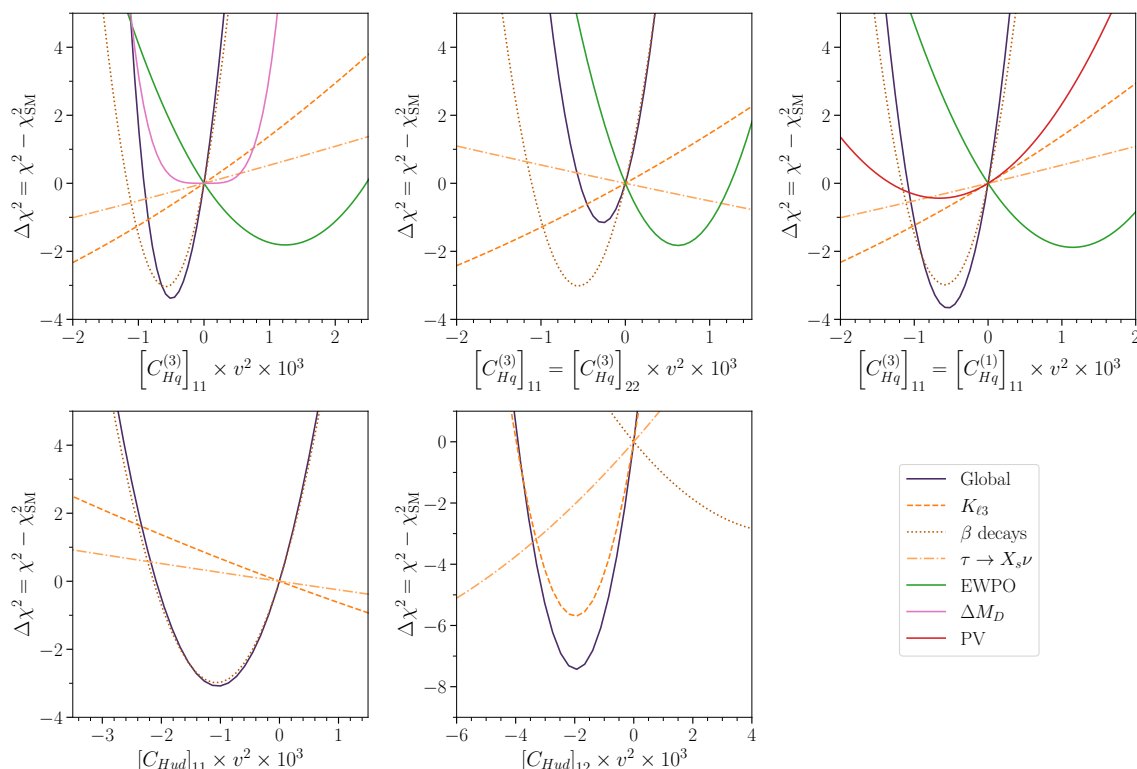
Figure 5. $\Delta\chi^2$ w.r.t. the SM as a function of the values of the Wilson coefficients for the 1D scenarios considered in the main text.
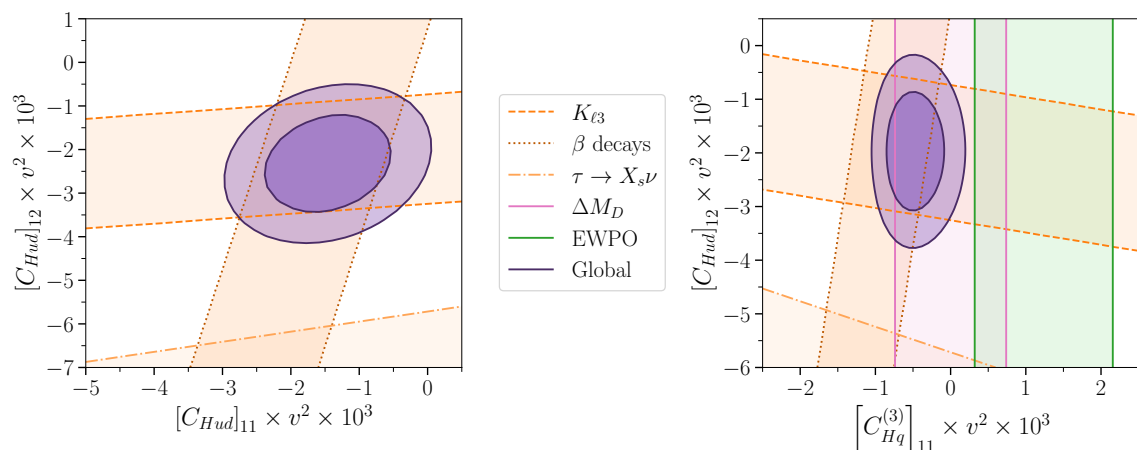

Figure 6. Preferred regions for our two 2-D scenarios, see main text for details.

W-u-s couplings. The resulting preferred regions are shown on the right of figure 6. The best fit points of these two dimensional scenarios together with the pulls are given in table 4.

3-D scenario. Here we consider the modifications induced if $\left[C_{Hq}^{(3)}\right]_{11}$, $[C_{Hud}]_{11}$, and $[C_{Hud}]_{12}$ are simultaneously non-zero. The results are shown in figure 7 from where we see that, similar to our 2-D scenarios, there is a strong preference for NP here, but also the
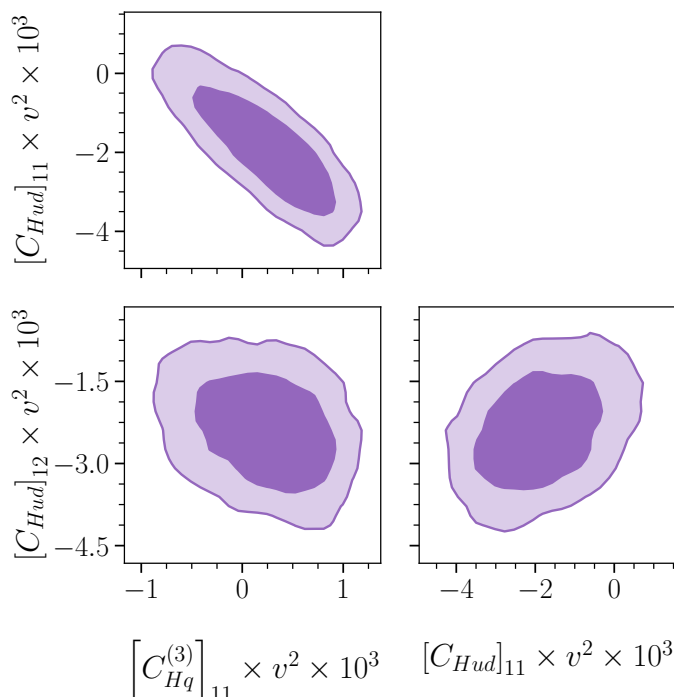
Figure 7. Global fit to our 3-D scenario with non-zero Wilson coefficients $\left[C^{(3)}_{Hq}\right]_{11}$, $[C_{Hud}]_{11}$, and $[C_{Hud}]_{12}$.

significant correlation between left-handed and right-handed W-u-d modifications. In the appendix D, we consider the 4-D scenarios in which we avoid or weaken the bounds from D^0–$\overline{D}^0$ mixing by adding $\left[C^{(3)}_{Hq}\right]_{11}$ or a $\left[C^{(3)}_{Hq}\right]_{22}$ as free parameters. However, the situation does not change significantly compared to the 3-D scenario as can also be seen from the pulls given in table 4.

Summary. The scenarios with modifications of right-handed W-u-s couplings provide the best improvement relative to the SM (which roughly agrees with the results in ref. [8]) and do not lead to problems in flavour physics or electroweak precision measurements since constraints from $\text{SU}(2)_L$ invariance are not present. The scenarios with both left-handed and right-handed modifications displays a slightly larger $\Delta\chi^2$ (which can be understood by the fact left-handed operators change the EW fit by modifying Z-quark couplings) as summarized in table 4.

4.2 Vector-like quark models

Now we examine VLQs coupling to first and second generation quarks in general, and the representations providing a potential solution to the tensions in the CKM matrix in particular.[9] We fix the masses of the VLQs to $2\,\text{TeV}$, which is compatible with LHC searches [132–135] (a recent study has shown that the high-luminosity LHC could exclude a first generation U VLQ at this mass for $\xi^U_1 \gtrsim 0.25$ [136]). Note that the scaling of the

---

[9]For a recent analysis of VLQs coupling to third generation quarks we refer the interested reader to ref. [56].

EFT Scenario	Best fit point	$-\Delta\chi^2$	Pull
$\left[C_{Hq}^{(3)}\right]_{11}$	-0.50	3.3	$1.8\,\sigma$
$\left[C_{Hq}^{(3)}\right]_{11} = \left[C_{Hq}^{(3)}\right]_{22}$	-0.27	1.1	$1.1\,\sigma$
$\left[C_{Hq}^{(3)}\right]_{11} = \left[C_{Hq}^{(1)}\right]_{11}$	-0.55	3.7	$1.9\,\sigma$
$[C_{Hud}]_{11}$	-1.0	3.1	$1.8\,\sigma$
$[C_{Hud}]_{12}$	-2.0	7.4	$2.7\,\sigma$
$([C_{Hud}]_{11}, [C_{Hud}]_{12})$	$(-1.4, -2.1)$	13	$3.2\,\sigma$
$\left(\left[C_{Hq}^{(3)}\right]_{11}, [C_{Hud}]_{12}\right)$	$(-0.43, -2.0)$	11	$2.8\,\sigma$
$\left(\left[C_{Hq}^{(3)}\right]_{11}, [C_{Hud}]_{11}, [C_{Hud}]_{12}\right)$	$(0.27, -1.9, -2.4)$	16	$2.9\,\sigma$
$\left(\left[C_{Hq}^{(3)}\right]_{11}, \left[C_{Hq}^{(3)}\right]_{22}, [C_{Hud}]_{11}, [C_{Hud}]_{12}\right)$	$(0.59, 0.76, -2.6, -2.5)$	17	$2.9\,\sigma$
$\left(\left[C_{Hq}^{(3)}\right]_{11}, \left[C_{Hq}^{(1)}\right]_{11}, [C_{Hud}]_{11}, [C_{Hud}]_{12}\right)$	$(0.29, 0.11, -2.0, -2.4)$	13	$2.6\,\sigma$

Table 4. Best fit points, $\Delta\chi^2$ and pulls w.r.t. the SM hypothesis for the various EFT scenarios. The best fit points are in units of $10^{-3}v^{-2}$.

bounds (with the exception of $\Delta F = 2$ processes) is just proportional to coupling squared over mass squared, modulus logarithmic effects from the renormalization group evolution. For D^0–$\overline{D}^0$ and kaon mixing, we have included the one-loop matching which becomes relevant for larger masses and breaks the simple scaling observed in the other processes.

In the figures 8 to 13 we show in the left-handed panels the preferred regions assuming multiple generations of VLQs, coupling separately to first and second generations quarks, thus avoiding tree-level effects in kaon FCNC processes (despite effects from CKM rotations in D^0–$\overline{D}^0$ mixing). In the right-handed panels the same fit for a single LQ representations, coupling simultaneously to first and second generations quarks is shown. Here, as explained in section 3.3, "CKM" stands for the combined region from the observables listed in tables 5 to 8 as well as from inclusive τ decay, while the "K FCNC" includes the observables listed in table 9. Let us now discuss the various representations separately.

U (figure 8). The $SU(2)_L$ singlet U (with quantum numbers of a right-handed up-type quark of the SM) leads to modified left-handed W coupling to quarks, so that the CKM tensions favour a non-zero first generation coupling. However, EW precision measurements and data from PV experiments limit the possible size of this coupling, even in the absence of direct contributions to D^0–$\overline{D}^0$ mixing (left panel). In the right panel, the best fit point is at $\xi_1^U = -0.2, \xi_2^U = 0.045$ with a pull w.r.t. the SM of $2.2\,\sigma$.

D (figure 9). The allowed regions for the Yukawa couplings of D (which has the quantum numbers of a right-handed down-type quark in the SM). We see that while for a single generation kaon FCNC constraints are very severe, (right panel) while in the situation with
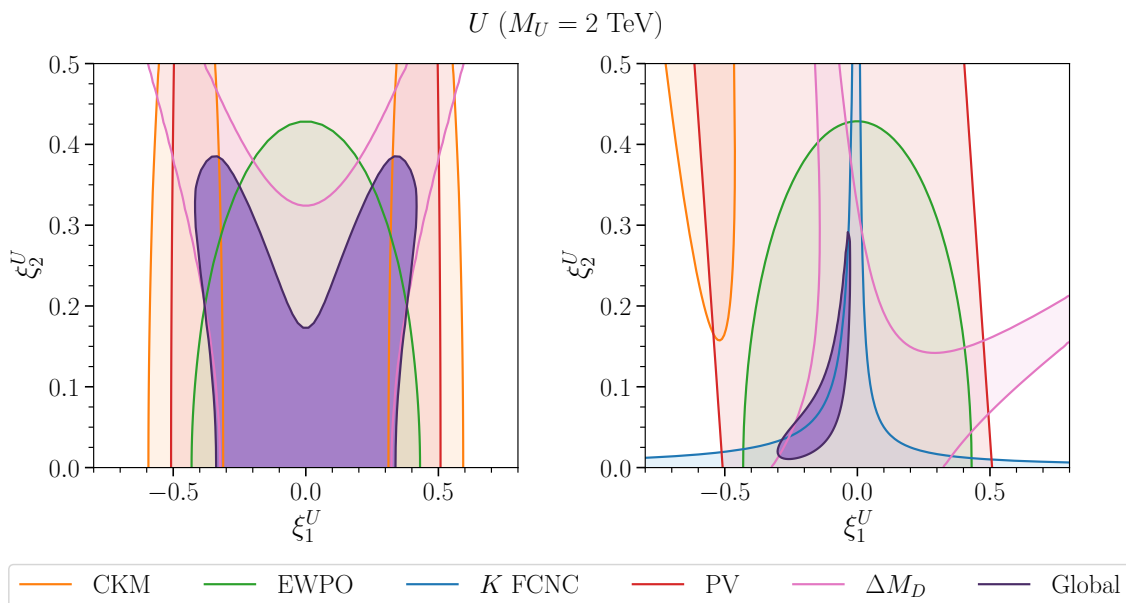
Figure 8. Global fit to 1st and 2st generation couplings of the VLQ U. The left-hand side assumes multiple generations of VLQs, each only coupling to a single generation (i.e. effectively removing constraints from kaon physics), while on the right side this assumption is removed.

two generations the allowed regions are much more sizable (left panel). We see that in either case, the data favours a single non-zero coupling, with a best fit at $\xi_1^D = -0.34$ and a one-dimensional pull w.r.t. the SM of $1.8\,\sigma$.

Q_5 (figure 10). This $\text{SU}(2)_L$ doublet VLQ with exotic hypercharge only generates modified Z couplings (but no W couplings) at tree-level, and hence there is no sensitivity to the CKM anomalies. In fact, as the modifications are only to the right-handed Z-d-d couplings, the current bounds on this VLQ are very weak, as can be seen in the left-hand side of the figure. While PV provides some bounds, there is a small preference for non-zero couplings from EW precision measurements due to the current small tensions in Z width and hadronic cross-section results. Once we allow for a single VLQ to couple to both generations however, we find that kaon physics drastically reduces the allowed region — this occurs due to the RG and matrix element enhancement of $(\bar{s}\gamma^\mu P_L d)(\bar{s}\gamma_\mu P_R d)$ four-quark operators in ϵ_K.

Q_7 (figure 11). The results for this VLQ are very similar to the ones for Q_5, even though this VLQ modifies right-handed Z-u-u couplings, instead of Z-d-d ones, although now the main bounds, in case it couples to both first and second generation, originate from D^0–$\bar{\text{D}}^0$ mixing.

T_1 (figure 12). This $\text{SU}(2)_L$ triplet modifies the left-handed charged current, thus affecting the CKM determinations, but in the wrong direction to resolve the first-row unitarity deviations. Therefore, the CKM measurements merely provide a constraint on its interactions, alongside D^0–$\bar{\text{D}}^0$ mixing and parity violation. The modifications to Z-quark couplings
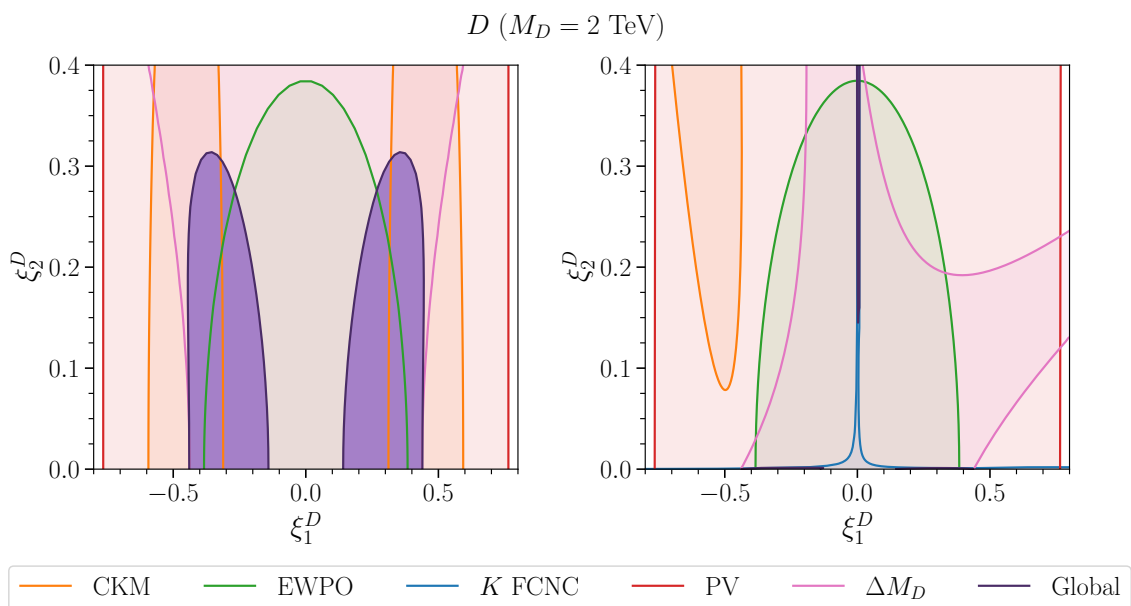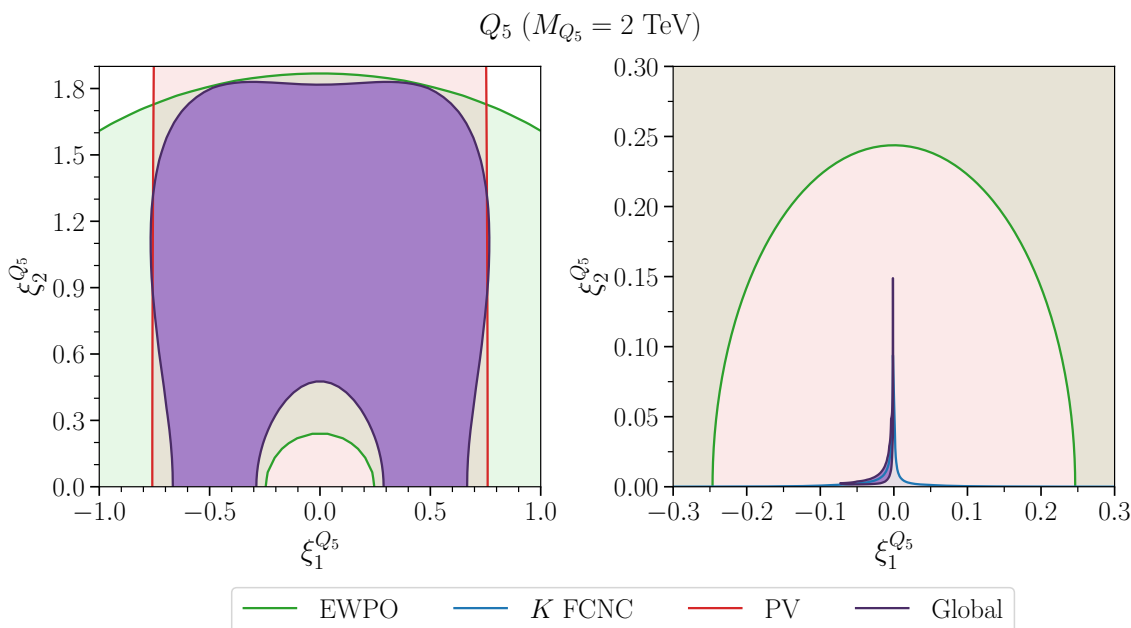
Figure 9. Global fit to 1$^{\text{st}}$ and 2$^{\text{st}}$ generation couplings of the VLQ D. The left-hand side assumes multiple generations of VLQs, each only coupling to a single generation (i.e. effectively removing constraints from kaon physics), while on the right side this assumption is removed.
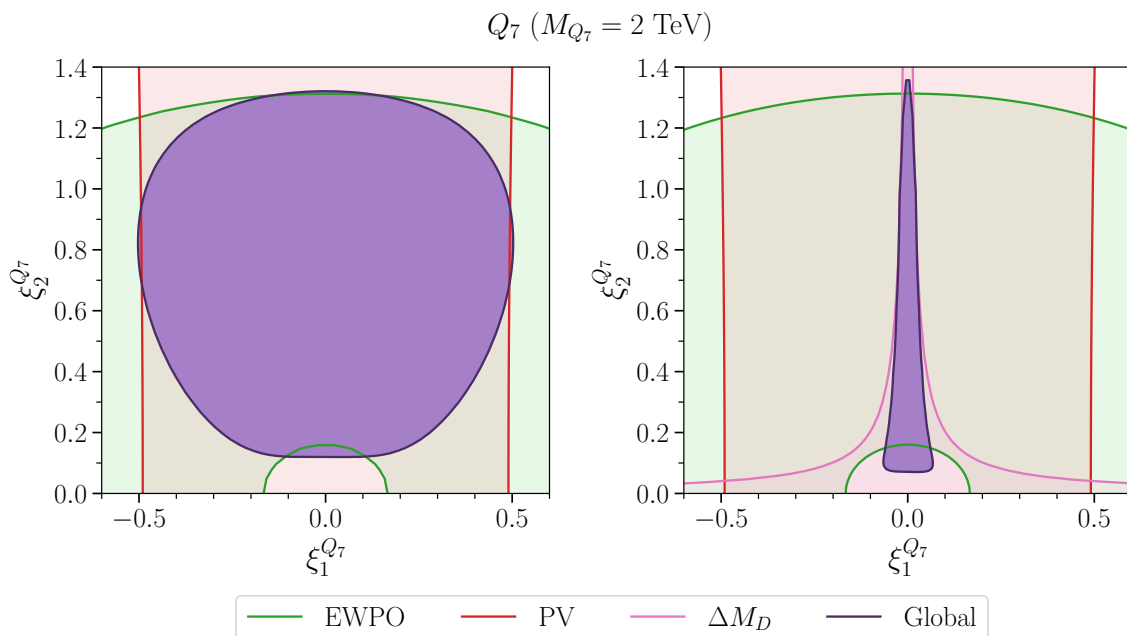

Figure 10. Global fit to 1$^{\text{st}}$ and 2$^{\text{st}}$ generation couplings of the VLQ Q_5. The left-hand side assumes multiple generations of VLQs, each only coupling to a single generation (i.e. effectively removing constraints from kaon physics), while on the right side this assumption is removed.

Figure 11. Global fit to 1$^{\text{st}}$ and 2$^{\text{st}}$ generation couplings of the VLQ Q_7. The left-hand side assumes multiple generations of VLQs, each only coupling to a single generation (i.e. effectively removing constraints from kaon physics), while on the right side this assumption is removed.

are smaller than in case of the SU(2)$_L$ singlet VLQs, and so the corresponding bounds cannot be seen in our region shown. Once we allow the triplet to couple to both generations at once, D^0–$\overline{\text{D}}^0$ mixing becomes stronger and kaon constraints are extremely tight.

T_2 (figure 13). The other triplet T_2 has essentially the same bounds as the first, but bounds from low-energy parity violation are slightly stronger while D^0–$\overline{\text{D}}^0$ mixing slightly weaker. Again, once we include couplings to both generations of a single VLQ, kaon decays prove to be very strong and the globally allowed region is quite small.

Q (figure 14). For the SU(2)$_L$ doublet Q, since it can have both couplings to right-handed up and down quarks, we instead show two fits, for either purely 1$^{\text{st}}$ or purely 2$^{\text{nd}}$ generation down quark interactions. The Q doublet is unique in generating modifications to the right-handed W couplings and, as expected from our previous EFT results, there is a strong preference towards non-zero couplings to both right-handed u and d (left) or u and s (right). However, unlike in our simple EFT scenario, the Q field generates additional correlated effects in Z couplings through SU(2) invariance, and so PV and EWPO partially limit the parameter space. In the left panel, the best fit point is $\xi_1^u = -0.29$, $\xi_1^d = 0.21$ and has a pull w.r.t. the SM of $1.1\,\sigma$. For the right panel, we find a best fit at $\xi_1^u = -0.33$, $\xi_2^d = 0.38$ and a pull of $2.1\,\sigma$.

VLQs and tensions in the Cabibbo angle. In our SMEFT analysis we saw that resolving the CAA via modified gauge boson couplings requires NP in $\left[C_{Hq}^{(3)}\right]_{11}$ and/or $[C_{Hud}]_{11}$ as well as in $[C_{Hud}]_{12}$ for the V_{us} tension. From the tree-level matching of VLQs on the SMEFT (see eq. (3.6)), we see that only the SU(2)$_L$ doublet Q can generate
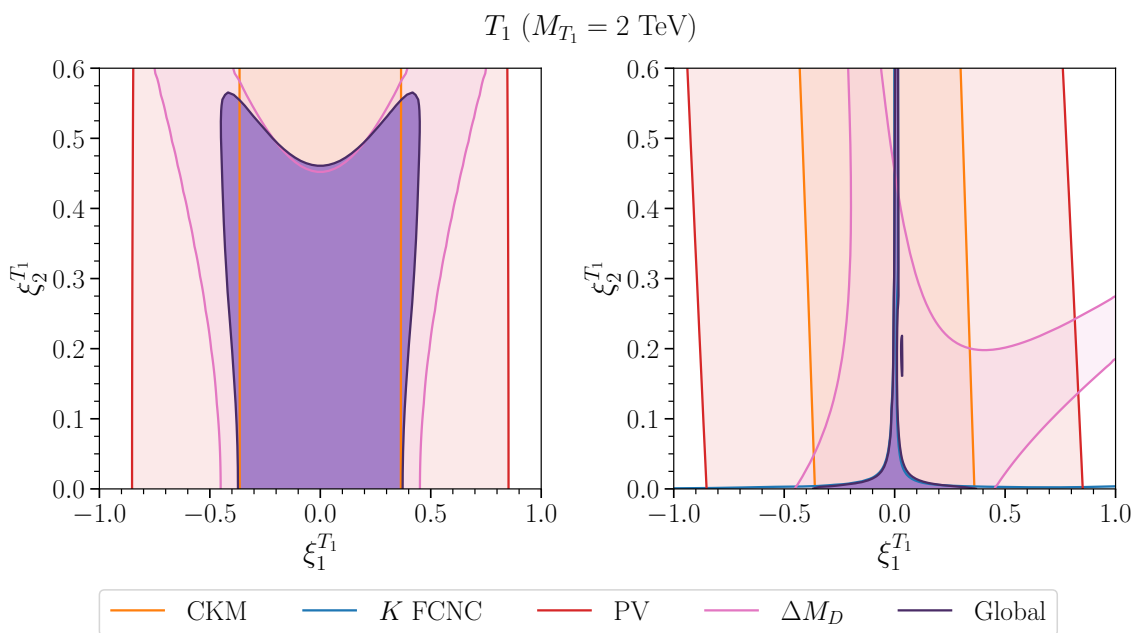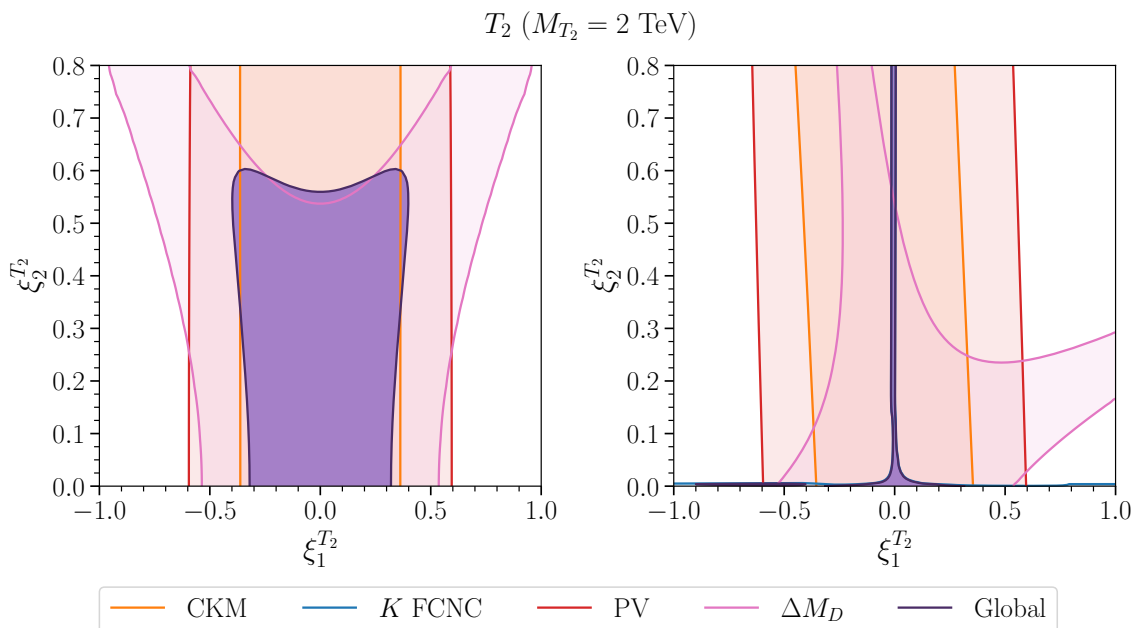
T_1 $(M_{T_1} = 2 \text{ TeV})$

| CKM | K FCNC | PV | ΔM_D | Global |

Figure 12. Global fit to 1$^{\text{st}}$ and 2$^{\text{st}}$ generation couplings of the VLQ T_1. The left-hand side assumes multiple generations of VLQs, each only coupling to a single generation (i.e. effectively removing constraints from kaon physics), while on the right side this assumption is removed.
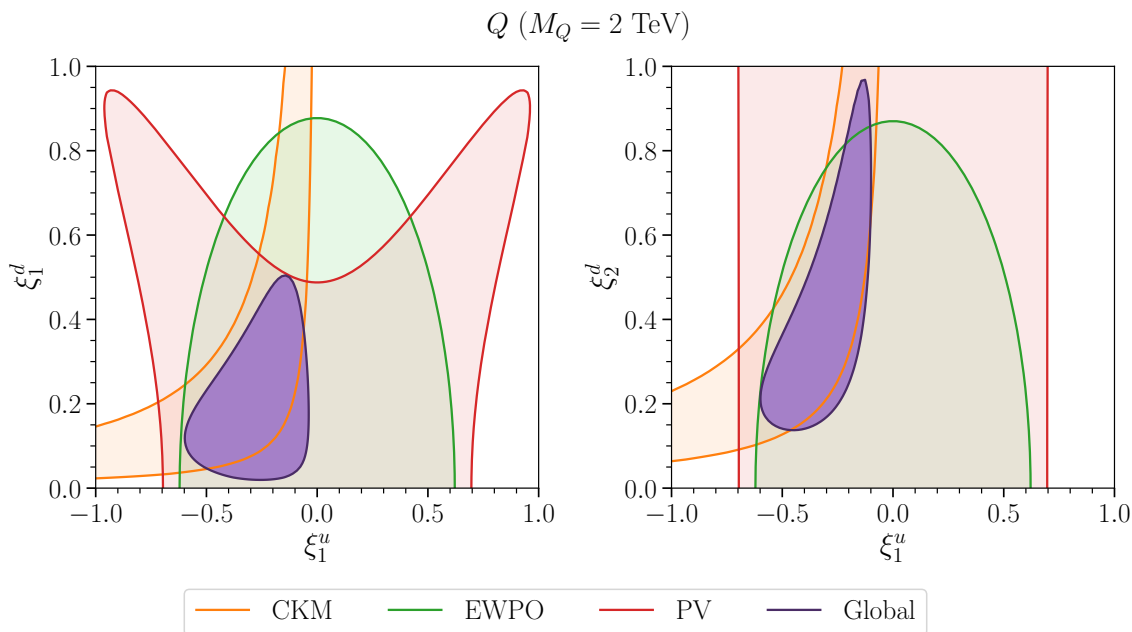

T_2 $(M_{T_2} = 2 \text{ TeV})$

| CKM | K FCNC | PV | ΔM_D | Global |

Figure 13. Global fit to 1$^{\text{st}}$ and 2$^{\text{st}}$ generation couplings of the VLQ T_2. The left-hand side assumes multiple generations of VLQs, each only coupling to a single generation (i.e. effectively removing constraints from kaon physics), while on the right side this assumption is removed.

Figure 14. Preferred regions for the VLQ Q with either couplings to u and d (left) or u and s (right).

the coefficients C_{Hud} that generate right-handed W couplings. Furthermore, for a single generation of the doublet, NP in the right-handed W-u-d and W-u-s vertices (at the same time) lead to significant NP in right-handed Z-d-s couplings, stringently constrained by ϵ_K [122, 123]. Updating their result, we find that a single Q doublet coupled to both d and s would have to obey $M_Q/\sqrt{\xi_1^d \xi_2^d} > 175\,\text{TeV}$ to be consistent with experiment, and therefore far too heavy to be relevant to the CAA.

Thus, a full explanation of the tensions in the Cabibbo angle determination require a modified W-u-d and W-u-s coupling and thus multiple generations of Q. Similarly, one can solve the CAA via a modified left-handed W-u-d coupling and a right-handed W-u-s coupling which again requires at least two VLQs. This means that a full solution of the CAA demands the presence of at least two VLQs.

5   Conclusions

In this article we studied modified couplings of light quarks to EW gauge bosons, both in the SMEFT and in models with VLQs. We paid particular attention to the different determinations of the Cabibbo angle that are in disagreement with each other, pointing towards such modified W couplings to quarks. We performed a global analysis using `smelli`, taking into account the constraints for EW precision and flavour observables.

In more detail, we first summarised the current status of the determinations of the CKM elements V_{ud} and V_{us}. For V_{ud}, where super-allowed β decays continue to provide the most precise determination, neutron decays is quickly approaching competitively, and its current central value is only slightly larger than (and therefore perfectly consistent with) the one

from super-allowed decays. For the direct determination of V_{us} the leading decay mode is $K \to \pi \ell \nu$ as there are still questions to be resolved regarding theory prediction for inclusive τ decays and how this should be applied to data. Finally, the ratio V_{us}/V_{ud} is dominated by $K \to \mu\nu/\pi \to \mu\nu$ as the ratios $\tau \to K\nu/\tau \to \pi\nu$ and $K \to \pi\ell\nu/\pi \to \pi e\nu$ are currently limited by the experimental data. We tested the CKM unitarity prediction of the SM by taking each pair of the best measurements individually, and find that it is violated between $1.8\,\sigma$ and $3.3\,\sigma$ (see eq. (2.13)). This agrees with the result of the global fit to all available data where we find the unitarity violation at the $2.8\,\sigma$ level (see eq. (2.12)). Furthermore, a tension between the different determinations of V_{us} exists, which can only be explained by non-standard right-handed interactions and can be tested through a $K \to \pi\mu\nu/K \to \mu\nu$ measurement in the near future by NA62 [19].

In our global SMEFT fit, we found that several scenarios can solve or alleviate the tensions in the determinations of the Cabibbo angle, as summarized in table 4. The simplest and least problematic case is that of right-handed charged currents (both in W-u-d and W-u-s couplings) which can bring all the main determinations into agreement without being in conflict with EW precision or flavour observables, and is therefore favoured over the SM hypothesis by $3.2\,\sigma$ ($2.7\,\sigma$) in the best 2-D (1-D) scenario. Other scenarios with modified left-handed charged currents (only) are also preferred over the SM hypothesis, but cannot account for the discrepancies within V_{us} and face constraints from EW precision measurements as well as D^0–$\overline{D}^0$ mixing. While the latter bounds can be weakened or avoided by considering a U(2) flavour symmetry or a specific combination of Wilson coefficients, respectively, the global fit displays a maximal pull of 1.9σ if only left-handed currents are considered.

The most natural extension of the SM that leads to modified EW gauge couplings to quarks are VLQs. They affect these couplings already at tree-level and are also theoretically well-motivated, e.g., by grand unified theories, composite and extra-dimensional models and little Higgs models etc. We first matched the different VLQ representations under the SM gauge group on the SMEFT (at tree-level for the charged current and EW precision observables and at loop-level for $\Delta F = 2$ processes) and used these results to calculate the relevant effects in the related observables. We then performed a global fit for the different representations of VLQs, taking into account couplings to first and second generation quarks. While a single VLQ coupling simultaneously to first and second generation quarks will lead to FCNCs and is hence very constrained, these bounds can be avoided or weakened for multiple generations of VLQs.

The SU(2)$_L$ singlet VLQs can improve the fit w.r.t. the CAA, but EW precision and D^0–$\overline{D}^0$ mixing (as well as PV measurements for the U) prevent a better description of data. The SU(2)$_L$ triplet VLQs generate the wrong sign to match our left-handed EFT scenario for the CAA, so that here CKM unitarity acts as a constraint but the tension cannot be explained. The SU(2)$_L$ doublets with non-SM-like hypercharges do not contribute to CKM observables, as they only generate modified Z but not W couplings to quarks. The heavy SM-like doublet Q proves the most interesting case, as this is the only VLQ that generates the right-handed W couplings to quarks. As expected from our EFT fits, this VLQ is strongly favoured by the CKM measurements, but now faces bounds from EWPO and PV as modified right-handed Z couplings to quarks are also induced, removing some of

the parameter space and reducing the improvement to the χ^2 of the fit to data. In fact, if one compares the $[C_{Hud}]_{11}$ scenario with a best fit pull of $1.8\,\sigma$ to the corresponding Q UV model with only $1.1\,\sigma$, and similarly the $[C_{Hud}]_{12}$ scenario has a best fit pull of $2.7\,\sigma$, compared to only $2.1\,\sigma$ in the second Q scenario. We note however the best fit points remains consistent with the right-handed EFT fit.

In conclusion, the tensions related to the determination of the Cabibbo angle can be most easily explained by new physics leading to right-handed charged currents and therefore by vector-like quark Q. Therefore, while collider bounds for third generations VLQs have been well studied, the CAA provides strong motivation for searches for VLQs coupling to first and second generation quarks.

Acknowledgments

A   SMEFT matching

Here we present the matching expressions at one-loop for the four-quarks operators which contribute to D^0–$\overline{D}^0$ mixing, which we calculated using `matchmakereft` [137].[10]

$$
\begin{aligned}
\left[C_{qq}^{(1)}\right]_{ijkl} = &-\frac{\xi_{fi}^{U*}\xi_{fj}^{U}\xi_{gk}^{U*}\xi_{gl}^{U}}{256\pi^2 M_U^2} + \frac{3(Y^uY^{u,\dagger})_{ij}\xi_{fk}^{U*}\xi_{fl}^{U}}{512\pi^2 M_U^2} + \frac{3(Y^uY^{u,\dagger})_{kl}\xi_{fi}^{U*}\xi_{fj}^{U}}{512\pi^2 M_U^2} \\
&-\frac{\xi_{fi}^{D*}\xi_{fj}^{D}\xi_{gk}^{D*}\xi_{gl}^{D}}{256\pi^2 M_D^2} - \frac{3(Y^uY^{u,\dagger})_{ij}\xi_{fk}^{D*}\xi_{fl}^{D}}{512\pi^2 M_D^2} - \frac{3(Y^uY^{u,\dagger})_{kl}\xi_{fi}^{D*}\xi_{fj}^{D}}{512\pi^2 M_D^2} \\
&-\frac{9\xi_{i}^{T_1*}\xi_{j}^{T_2}\xi_{k}^{T_1*}\xi_{l}^{T_2}}{4096\pi^2 M_{T_1}^2} - \frac{9(Y^uY^{u,\dagger})_{ij}\xi_{fk}^{T_1*}\xi_{fl}^{T_1}}{2048\pi^2 M_{T_1}^2} - \frac{9(Y^uY^{u,\dagger})_{kl}\xi_{fi}^{T_1*}\xi_{fj}^{T_1}}{2048\pi^2 M_{T_1}^2} \\
&-\frac{9\xi_{fi}^{T_2*}\xi_{fj}^{T_2}\xi_{gk}^{T_2*}\xi_{gl}^{T_2}}{4096\pi^2 M_{T_2}^2} + \frac{9(Y^uY^{u,\dagger})_{ij}\xi_{fk}^{T_2*}\xi_{fl}^{T_2}}{2048\pi^2 M_{T_2}^2} + \frac{9(Y^uY^{u,\dagger})_{kl}\xi_{fi}^{T_2*}\xi_{fj}^{T_2}}{2048\pi^2 M_{T_2}^2},
\end{aligned}
\tag{A.1}
$$

---

[10]A partial calculation of the one-loop matching was done in [37] for the D, Q, Q_5, T_1, and T_2 VLQs.

$$\left[C_{qq}^{(3)}\right]_{ijkl} = -\frac{\xi_{fi}^{U*}\xi_{fj}^{U}\xi_{gk}^{U*}\xi_{gl}^{U}}{256\pi^2 M_U^2} + \frac{3(Y^u Y^{u,\dagger})_{ij}\xi_{fk}^{U*}\xi_{fl}^{U}}{512\pi^2 M_U^2} + \frac{3(Y^u Y^{u,\dagger})_{kl}\xi_{fi}^{U*}\xi_{fj}^{U}}{512\pi^2 M_U^2} \qquad (A.2)$$

$$-\frac{\xi_{fi}^{D*}\xi_{fj}^{D}\xi_{gk}^{D*}\xi_{gl}^{D}}{256\pi^2 M_D^2} + \frac{3(Y^u Y^{u,\dagger})_{ij}\xi_{fk}^{D*}\xi_{fl}^{D}}{512\pi^2 M_D^2} + \frac{3(Y^u Y^{u,\dagger})_{kl}\xi_{fi}^{D*}\xi_{fj}^{D}}{512\pi^2 M_D^2}$$

$$-\frac{\xi_{fi}^{T_1*}\xi_{fj}^{T_2}\xi_{gk}^{T_1*}\xi_{gl}^{T_2}}{4096\pi^2 M_{T_1}^2} - \frac{3(Y^u Y^{u,\dagger})_{ij}\xi_{fk}^{T_1*}\xi_{fl}^{T_1}}{2048\pi^2 M_{T_1}^2} - \frac{3(Y^u Y^{u,\dagger})_{kl}\xi_{fi}^{T_1*}\xi_{fj}^{T_1}}{2048\pi^2 M_{T_1}^2}$$

$$-\frac{\xi_{fi}^{T_2*}\xi_{fj}^{T_2}\xi_{gk}^{T_2*}\xi_{gl}^{T_2}}{4096\pi^2 M_{T_2}^2} - \frac{3(Y^u Y^{u,\dagger})_{ij}\xi_{fk}^{T_2*}\xi_{fl}^{T_2}}{2048\pi^2 M_{T_2}^2} - \frac{3(Y^u Y^{u,\dagger})_{kl}\xi_{fi}^{T_2*}\xi_{fj}^{T_2}}{2048\pi^2 M_{T_2}^2},$$

$$\left[C_{qu}^{(1)}\right]_{ijkl} = -\frac{3(Y^{u,\dagger}Y^u)_{kl}\xi_{fi}^{U*}\xi_{fj}^{U}}{128\pi^2 M_U^2} - \frac{Y_{il}^u Y_{kj}^{u,\dagger}\xi_{fm}^{U*}\xi_{fm}^{U}}{96\pi^2 M_U^2} + \frac{3(Y^{u,\dagger}Y^u)_{kl}\xi_{fi}^{D*}\xi_{fj}^{D}}{128\pi^2 M_D^2} \qquad (A.3)$$

$$+\frac{Y_{il}^u \xi_{fj}^{D}(Y^{u,\dagger}\xi^{D\dagger})_{kf}}{192\pi^2 M_D^2} + \frac{\xi_{fi}^{D*}Y_{kj}^{u,\dagger}(\xi^D Y^u)_{fl}}{192\pi^2 M_D^2} - \frac{Y_{il}^u Y_{kj}^{u,\dagger}\xi_{fm}^{D*}\xi_{fm}^{D}}{96\pi^2 M_D^2}$$

$$-\frac{3(Y^u Y^{u,\dagger})_{ij}\xi_{fk}^{u*}\xi_{fl}^{u}}{128\pi^2 M_Q^2} - \frac{Y_{il}^u Y_{jk}^{u,\dagger}\xi_{fm}^{d*}\xi_{fm}^{d}}{96\pi^2 M_Q^2} - \frac{Y_{il}^u Y_{jk}^{u,\dagger}\xi_{fm}^{u*}\xi_{fm}^{u}}{96\pi^2 M_Q^2} - \frac{\xi_{fm}^{Q_5}\xi_{fm}^{Q_5*}Y_{il}^u Y_{kj}^{u,\dagger}}{96\pi^2 M_{Q_5}^2}$$

$$+\frac{3(Y^u Y^{u,\dagger})_{ij}\xi_{fk}^{Q_7*}\xi_{fl}^{Q_7}}{128\pi^2 M_{Q_7}^2} - \frac{Y_{il}^u(\xi^{Q_7}Y^{u,\dagger})_{fj}\xi_{fk}^{Q_7*}}{192\pi^2 M_{Q_7}^2} - \frac{(Y^u\xi^{Q_7\dagger})_{fi}Y^{u,\dagger})_{kj}\xi_{fl}^{Q_7}}{192\pi^2 M_{Q_7}^2}$$

$$-\frac{\xi_{fm}^{Q_7}\xi_{fm}^{Q_7*}Y_{il}^u Y_{kj}^{u,\dagger}}{96\pi^2 M_{Q_7}^2}$$

$$+\frac{9(Y^{u,\dagger}Y^u)_{kl}\xi_{fi}^{T_1*}\xi_{fj}^{T_1}}{512\pi^2 M_{T_1}^2} - \frac{Y_{il}^u \xi_{fj}^{D}(Y^{u,\dagger}\xi^{T_1\dagger})_{kf}}{256\pi^2 M_{T_1}^2} - \frac{\xi_{fi}^{T_1*}Y_{kj}^{u,\dagger}(\xi^{T_1}Y^u)_{fl}}{256\pi^2 M_{T_1}^2}$$

$$-\frac{Y_{il}^u Y_{kj}^{u,\dagger}\xi_{fm}^{T_1*}\xi_{fm}^{T_1}}{128\pi^2 M_{T_1}^2} - \frac{9(Y^{u,\dagger}Y^u)_{kl}\xi_{fi}^{T_2*}\xi_{fj}^{T_2}}{512\pi^2 M_{T_2}^2} - \frac{Y_{il}^u Y_{kj}^{u,\dagger}\xi_{fm}^{T_2*}\xi_{fm}^{T_2}}{128\pi^2 M_{T_2}^2},$$

$$\left[C_{qu}^{(8)}\right]_{ijkl} = -\frac{Y_{il}^u Y_{kj}^{u,\dagger}\xi_{fm}^{U*}\xi_{fm}^{U}}{16\pi^2 M_U^2} \qquad (A.4)$$

$$+\frac{Y_{il}^u \xi_{fj}^{D}(Y^{u,\dagger}\xi^{D\dagger})_{kf}}{32\pi^2 M_D^2} + \frac{\xi_{fi}^{D*}Y_{kj}^{u,\dagger}(\xi^D Y^u)_{fl}}{32\pi^2 M_D^2} - \frac{Y_{il}^u Y_{kj}^{u,\dagger}\xi_{fm}^{D*}\xi_{fm}^{D}}{16\pi^2 M_D^2}$$

$$-\frac{Y_{il}^u Y_{jk}^{u,\dagger}\xi_{fm}^{d*}\xi_{fm}^{d}}{16\pi^2 M_Q^2} - \frac{Y_{il}^u Y_{jk}^{u,\dagger}\xi_{fm}^{u*}\xi_{fm}^{u}}{16\pi^2 M_Q^2} - \frac{\xi_{fm}^{Q_5}\xi_{fm}^{Q_5*}Y_{il}^u Y_{kj}^{u,\dagger}}{16\pi^2 M_{Q_5}^2}$$

$$-\frac{Y_{il}^u(\xi^{Q_7}Y^{u,\dagger})_{fj}\xi_{fk}^{Q_7*}}{32\pi^2 M_{Q_7}^2} - \frac{(Y^u\xi^{Q_7\dagger})_{if}Y^{u,\dagger})_{kj}\xi_{fl}^{Q_7}}{32\pi^2 M_{Q_7}^2} - \frac{\xi_{fm}^{Q_7}\xi_{fm}^{Q_7*}Y_{il}^u Y_{kj}^{u,\dagger}}{16\pi^2 M_{Q_7}^2}$$

$$+\frac{Y_{il}^u \xi_{fj}^{T_1}(Y^{u,\dagger}\xi^{T_1\dagger})_{kf}}{128\pi^2 M_{T_1}^2} + \frac{\xi_{fi}^{T_1*}Y_{kj}^{u,\dagger}(\xi^{T_1}Y^u)_{fl}}{128\pi^2 M_{T_1}^2} - \frac{Y_{il}^u Y_{kj}^{u,\dagger}\xi_{fm}^{T_1*}\xi_{fm}^{T_1}}{64\pi^2 M_{T_1}^2}$$

$$-\frac{3Y_{il}^u Y_{kj}^{u,\dagger}\xi_{fm}^{T_2*}\xi_{fm}^{T_2}}{64\pi^2 M_{T_2}^2},$$

$$[C_{uu}]_{ijkl} = -\frac{\xi_{fi}^{u*}\xi_{fj}^{u}\xi_{gk}^{u*}\xi_{gl}^{u}}{64\pi^2 M_Q^2} + \frac{3(Y^{u,\dagger}Y^u)_{ij}\xi_{fk}^{u*}\xi_{fl}^{u}}{128\pi^2 M_Q^2} + \frac{3(Y^{u,\dagger}Y^u)_{kl}\xi_{fi}^{u*}\xi_{fj}^{u}}{128\pi^2 M_Q^2}$$
$$- \frac{\xi_{fi}^{q7*}\xi_{fj}^{Q7}\xi_{gk}^{Q7*}\xi_{gl}^{Q7}}{64\pi^2 M_{Q7}^2} - \frac{3(Y^{u,\dagger}Y^u)_{ij}\xi_{fk}^{Q7*}\xi_{fl}^{Q7}}{128\pi^2 M_{Q7}^2} - \frac{3(Y^{u,\dagger}Y^u)_{kl}\xi_{fi}^{Q7*}\xi_{fj}^{Q7}}{128\pi^2 M_{Q7}^2}, \tag{A.5}$$

where f, g are flavour indices for the new VLQs, we have assumed equal masses for multiple generations of VLQs to simplify the loop functions, and the matching conditions have been specified at the VLQ mass scale, such that $\ln(\mu^2/M^2)$ terms vanish.

In the down-basis we have adopted, it is useful to note that products of Yukawa matrices can be simplified as

$$\left(Y^u Y^{u,\dagger}\right)_{ij} = y_t^2 V_{3i}^* V_{3j} + \mathcal{O}\left(y_c^2\right), \quad \left(Y^{u,\dagger}Y^u\right)_{ij} = y_t^2 \delta_{3i}\delta_{3j} + \mathcal{O}\left(y_c^2\right). \tag{A.6}$$

Note though that we keep the full expressions in our numerical analyses.

B Effective CKM elements

In the presence of non-zero SMEFT coefficients, the effective CKM elements as extracted from β decay, semi-leptonic kaon decay, and leptonic kaon and pion decay are:

$$V_{ud}^\beta = V_{ud} + v^2 \left[V_{\text{CKM}} \cdot C_{Hq}^{(3)}\right]_{11} + \frac{v^2}{2}\left[C_{Hud}\right]_{11}, \tag{B.1}$$

$$V_{us}^{K\ell3} = V_{us} + v^2 \left[V_{\text{CKM}} \cdot C_{Hq}^{(3)}\right]_{12} + \frac{v^2}{2}\left[C_{Hud}\right]_{12}, \tag{B.2}$$

$$V_{uq}^{M\mu2} = V_{uq} + v^2 \left[V_{\text{CKM}} \cdot C_{Hq}^{(3)}\right]_{1q} - \frac{v^2}{2}\left[C_{Hud}\right]_{1q}, \tag{B.3}$$

for $q = d, s$ and $M = K, \pi$ in the final equation. (Notice that we obviously see here how right-handed currents are needed to resolve the tension between V_{us} determinations.)

Rearranging, and assuming small NP contributions in only the four coefficients $\left[C_{Hq}^{(3)}\right]_{11,12}$ and $[C_{Hud}]_{11,12}$ we find:

$$V_{ud} = V_{ud}^\beta - v^2 \left(V_{ud}^\beta \left[C_{Hq}^{(3)}\right]_{11} + \frac{1}{2}\left[C_{Hud}\right]_{11}\right), \tag{B.4}$$

$$V_{us} = V_{us}^{K\ell3} - v^2 \left(V_{ud}^\beta \left[C_{Hq}^{(3)}\right]_{12} + \frac{1}{2}\left[C_{Hud}\right]_{12}\right), \tag{B.5}$$

$$\frac{V_{us}}{V_{ud}} = \frac{V_{us}^{K\mu2} - v^2 \left(V_{ud}\left[C_{Hq}^{(3)}\right]_{12} - \frac{1}{2}\left[C_{Hud}\right]_{12}\right)}{V_{ud}^{\pi\mu2} - v^2 \left(V_{ud}\left[C_{Hq}^{(3)}\right]_{11} - \frac{1}{2}\left[C_{Hud}\right]_{11}\right)} \tag{B.6}$$

$$= \left(\frac{V_{us}}{V_{ud}}\right)^{M\mu2} + v^2 \left(\left(\frac{V_{us}}{V_{ud}}\right)^{M\mu2}\left[C_{Hq}^{(3)}\right]_{11} - \left[C_{Hq}^{(3)}\right]_{12} - \left(\frac{V_{us}}{V_{ud}}\right)^{M\mu2}\frac{[C_{Hud}]_{11}}{2V_{ud}^\beta} + \frac{[C_{Hud}]_{12}}{2V_{ud}^\beta}\right). \tag{B.7}$$

C smelli observables

In tables 5 to 10 we list the observables shown in our global fits, along with the relevant experimental measurements and theory papers used in the computation.

Observable	Exp.	Theory	Observable	Exp.	Theory
$\mathrm{BR}(K_L \to \pi^+ e^+ \nu)$	[64]	[138, 139]	$\mathrm{BR}(K_S \to \pi^+ e^+ \nu)$	[84]	[138, 139]
$\mathrm{BR}(K^+ \to \pi^0 e^+ \nu)$	[64]	[138, 139]	$\mathrm{BR}(K_L \to \pi^+ \mu^+ \nu)$	[64]	[138, 139]
$\mathrm{BR}(K_S \to \pi^+ \mu^+ \nu)$	[83]	[138, 139]	$\mathrm{BR}(K^+ \to \pi^0 \mu^+ \nu)$	[64]	[138, 139]
$\ln(C)(K^+ \to \pi^0 \mu^+ \nu)$	[140]	[138, 139]	$R_T(K^+ \to \pi^0 \mu^+ \nu)$	[141]	[138, 139]

Table 5. The "$K_{\ell 3}$" observables used in smelli, along with the relevant experimental measurements and theory papers used in the computation.

Observable	Exp.	Theory	Observable	Exp.	Theory
$\mathcal{F}t(^{10}\mathrm{C})$	[63]	[142]	$\mathcal{F}t(^{14}\mathrm{O})$	[63]	[142]
$\mathcal{F}t(^{22}\mathrm{Mg})$	[63]	[142]	$\mathcal{F}t(^{26m}\mathrm{Al})$	[63]	[142]
$\mathcal{F}t(^{34}\mathrm{Cl})$	[63]	[142]	$\mathcal{F}t(^{34}\mathrm{Ar})$	[63]	[142]
$\mathcal{F}t(^{38m}\mathrm{K})$	[63]	[142]	$\mathcal{F}t(^{38}\mathrm{Ca})$	[63]	[142]
$\mathcal{F}t(^{42}\mathrm{Sc})$	[63]	[142]	$\mathcal{F}t(^{46}\mathrm{V})$	[63]	[142]
$\mathcal{F}t(^{50}\mathrm{Mn})$	[63]	[142]	$\mathcal{F}t(^{54}\mathrm{Co})$	[63]	[142]
$\mathcal{F}t(^{62}\mathrm{Ga})$	[63]	[142]	$\mathcal{F}t(^{74}\mathrm{Rb})$	[63]	[142]
τ_n	[68]	[142]	$\tilde{A}_n$	[69, 143, 144]	[142]
R_n	[145]	[142]	λ_{AB}	[146]	[142]
a_n	[142]	[142]	$\tilde{a}_n$	[147]	[142]
$\tilde{B}_n$	[142]	[142]	D_n	[142]	[142]

Table 6. The "beta" observables used in smelli, along with the relevant experimental measurements and theory papers used in the computation.

Observable	Exp.	Observable	Exp.
$\mathrm{BR}(\tau^+ \to \pi^+ \bar{\nu})$	[64]	$\mathrm{BR}(\tau^+ \to K^+ \bar{\nu})$	[64]

Table 7. The exclusive τ decays observables used in smelli, along with the relevant experimental measurements and theory papers used in the computation.

Observable	Exp.	Theory	Observable	Exp.	Theory
$\mathrm{BR}(D^+ \to e^+\nu_e)$	[64]		$\mathrm{BR}(D^+ \to \mu^+\nu_\mu)$	[64]	
$\mathrm{BR}(D^+ \to \tau^+\nu_\tau)$	[64]		$\mathrm{BR}(D_s \to e^+\nu_e)$	[64]	
$\mathrm{BR}(D_s \to \mu^+\nu_\mu)$	[64]		$\mathrm{BR}(D_s \to \tau^+\nu_\tau)$	[64]	
$\mathrm{BR}(D^0 \to \pi^-\mu^+\nu_\mu)$	[64]	[148]	$\mathrm{BR}(D^0 \to \pi^-e^+\nu_e)$	[64]	[148]
$\mathrm{BR}(D^0 \to K^-e^+\nu_e)$	[64]	[148]	$\mathrm{BR}(D^0 \to K^-\mu^+\nu_\mu)$	[64]	[148]
$\langle\mathrm{BR}\rangle(D^0 \to \pi^-e^+\nu_e)$	[149, 150]	[148]	$\mathrm{BR}(D^+ \to \pi^0\mu^+\nu_\mu)$	[64]	[148]
$\langle\mathrm{BR}\rangle(D^0 \to K^-e^+\nu_e)$	[149, 150]	[148]	$\mathrm{BR}(D^+ \to K^0\mu^+\nu_\mu)$	[64]	[148]
$\langle\mathrm{BR}\rangle(D^+ \to K^0e^+\nu_e)$	[149, 151]	[148]	$\mathrm{BR}(D^+ \to \pi^0e^+\nu_e)$	[64]	[148]
$\langle\mathrm{BR}\rangle(D^+ \to \pi^0e^+\nu_e)$	[149, 151]	[148]	$\mathrm{BR}(D^+ \to K^0e^+\nu_e)$	[64]	[148]

Table 8. The D decay observables used in `smelli`, along with the relevant experimental measurements and theory papers used in the computation. $\langle\mathrm{BR}\rangle$ are q^2-binned branching ratios.

Observable	Exp.	Theory	Observable	Exp.	Theory
$\mathrm{BR}(K^+ \to \pi^+\nu\bar\nu)$	[152]	[153–157]	$\mathrm{BR}(K_L \to \pi^0\nu\bar\nu)$	[158]	[153–157]
$\mathrm{BR}(K_L \to e^+e^-)$	[64]	[159–161]	$\mathrm{BR}(K_S \to e^+e^-)$	[64]	[159–161]
$\mathrm{BR}(K_L \to \mu^+\mu^-)$	[64]	[159–161]	$\mathrm{BR}(K_S \to \mu^+\mu^-)$	[162]	[159–161]
$|\epsilon_K|$	[64]	[163–166]			

Table 9. The "K FCNC" observables used in `smelli`, along with the relevant experimental measurements and theory papers used in the computation.

Observable	Exp.	Theory	Observable	Exp.	Theory
Γ_Z	[167]	[168, 169]	σ^0_{had}	[167]	[168, 169]
R^0_e	[167]	[168, 169]	R^0_μ	[167]	[168, 169]
R^0_τ	[167]	[168, 169]	$A^{0,e}_{\mathrm{FB}}$	[167]	[168]
$A^{0,\mu}_{\mathrm{FB}}$	[167]	[168]	$A^{0,\tau}_{\mathrm{FB}}$	[167]	[168]
A_e	[170]	[168]	A_μ	[170]	[168]
A_τ	[170]	[168]	R^0_b	[170]	[168, 169]
R^0_c	[170]	[168, 169]	$A^{0,b}_{\mathrm{FB}}$	[170]	[168]
$A^{0,c}_{\mathrm{FB}}$	[170]	[168]	A_b	[170]	[168]
A_c	[170]	[168]	m_W	[171, 172]	[168, 173, 174]
Γ_W	[64]	[168]	$\mathrm{BR}(W^\pm \to e^\pm\nu)$	[175]	[168]
$\mathrm{BR}(W^\pm \to \mu^\pm\nu)$	[175]	[168]	$\mathrm{BR}(W^\pm \to \tau^\pm\nu)$	[175]	[168]
$\mathrm{R}(W^+ \to cX)$	[64]	[168]	$\mathrm{R}_{\mu e}(W^\pm \to \ell^\pm\nu)$	[176]	[168]
$\mathrm{R}_{\tau e}(W^\pm \to \ell^\pm\nu)$	[177]	[168]	$\mathrm{R}_{\tau\mu}(W^\pm \to \ell^\pm\nu)$	[178]	[168]
A_s	[179]	[168]	R^0_{uc}	[64]	[168, 169]

Table 10. The EWPO observables used in `smelli`, along with the relevant experimental measurements and theory papers used in the computation.

D   Plots for 4-D EFT scenarios

As D^0–$\overline{D}^0$ mixing is a serious bound when considering left-handed modifications, we go beyond the 3-D scenario by allowing a U(2) flavour symmetry for $C_{Hq}^{(3)}$ as well as the possibility of cancellation between $C_{Hq}^{(3)}$ and $C_{Hq}^{(1)}$ in Z couplings to up quarks, as done earlier in our 1-D scenarios. We therefore performed a global fit to the two scenarios

1. $\left[C_{Hq}^{(3)}\right]_{11}$, $[C_{Hud}]_{11}$, $[C_{Hud}]_{12}$ plus $\left[C_{Hq}^{(3)}\right]_{22}$, with the results shown in figure 15

and

2. $\left[C_{Hq}^{(3)}\right]_{11}$, $[C_{Hud}]_{11}$, $[C_{Hud}]_{12}$ plus $\left[C_{Hq}^{(1)}\right]_{11}$, with the results shown in figure 16.
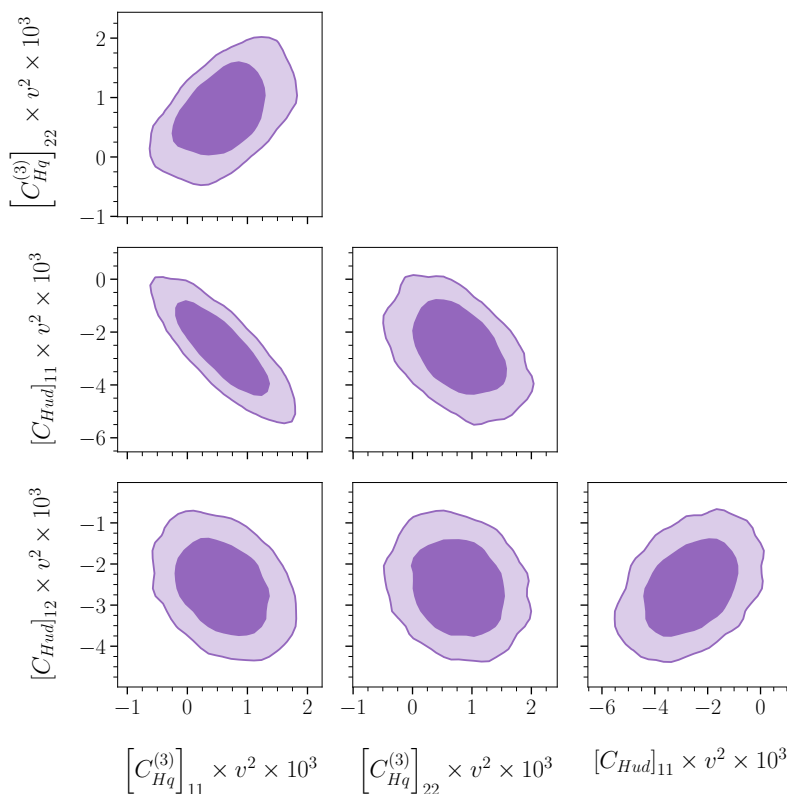
Figure 15. 4-D scenario with $\left[C_{Hq}^{(3)}\right]_{11}$, $\left[C_{Hq}^{(3)}\right]_{22}$, $[C_{Hud}]_{11}$, and $[C_{Hud}]_{12}$ being non-zero.
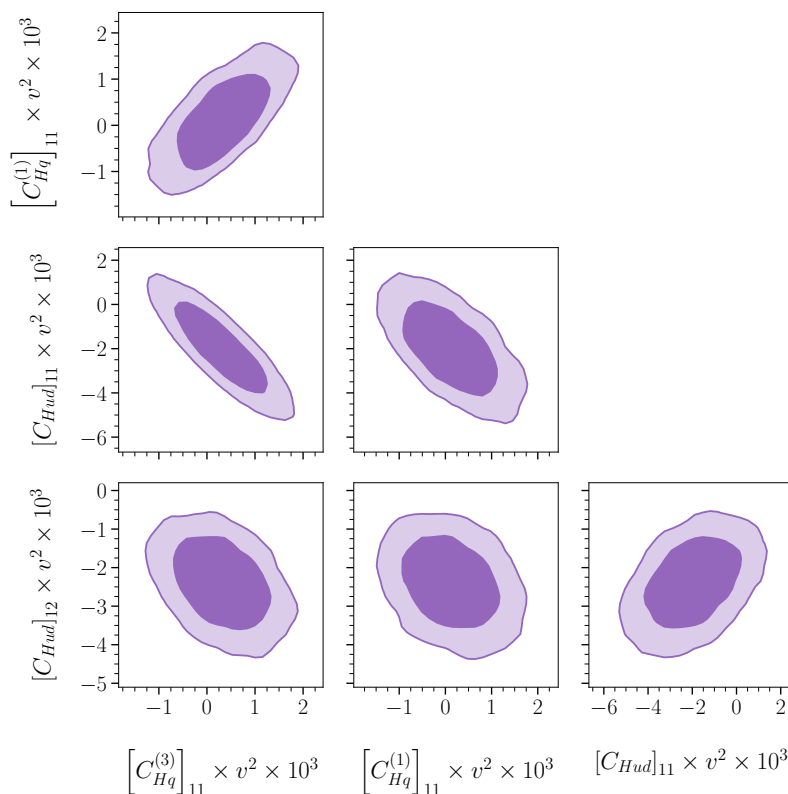
Figure 16. 4-D scenario with $\left[C_{Hq}^{(3)}\right]_{11}$, $\left[C_{Hq}^{(1)}\right]_{11}$, $[C_{Hud}]_{11}$, and $[C_{Hud}]_{12}$ being non-zero.

References

[1] ATLAS collaboration, *Observation of a new particle in the search for the Standard Model Higgs boson with the ATLAS detector at the LHC*, *Phys. Lett. B* **716** (2012) 1 [arXiv:1207.7214] [INSPIRE].

[2] CMS collaboration, *Observation of a New Boson at a Mass of 125 GeV with the CMS Experiment at the LHC*, *Phys. Lett. B* **716** (2012) 30 [arXiv:1207.7235] [INSPIRE].

[3] A. Crivellin and M. Hoferichter, *Hints of lepton flavor universality violations*, *Science* **374** (2021) 1051 [arXiv:2111.12739] [INSPIRE].

[4] A. Crivellin and J. Matias, *Beyond the Standard Model with Lepton Flavor Universality Violation*, in the proceedings of the *1st Pan-African Astro-Particle and Collider Physics Workshop*, (2022) [arXiv:2204.12175] [INSPIRE].

[5] O. Fischer et al., *Unveiling hidden physics at the LHC*, *Eur. Phys. J. C* **82** (2022) 665 [arXiv:2109.06065] [INSPIRE].

[6] M. Artuso, G. Isidori and S. Stone, *New Physics in b Decays*, World Scientific (2022) [DOI:10.1142/12696] [INSPIRE].

[7] B. Belfatto, R. Beradze and Z. Berezhiani, *The CKM unitarity problem: A trace of new physics at the TeV scale?*, *Eur. Phys. J. C* **80** (2020) 149 [arXiv:1906.02714] [INSPIRE].

[8] Y. Grossman, E. Passemar and S. Schacht, *On the Statistical Treatment of the Cabibbo Angle Anomaly*, *JHEP* **07** (2020) 068 [arXiv:1911.07821] [INSPIRE].

[9] C.-Y. Seng, X. Feng, M. Gorchtein and L.-C. Jin, *Joint lattice QCD-dispersion theory analysis confirms the quark-mixing top-row unitarity deficit*, *Phys. Rev. D* **101** (2020) 111301 [arXiv:2003.11264] [INSPIRE].

[10] A.M. Coutinho, A. Crivellin and C.A. Manzari, *Global Fit to Modified Neutrino Couplings and the Cabibbo-Angle Anomaly*, *Phys. Rev. Lett.* **125** (2020) 071802 [arXiv:1912.08823] [INSPIRE].

[11] C.A. Manzari, A.M. Coutinho and A. Crivellin, *Modified lepton couplings and the Cabibbo-angle anomaly*, *PoS* **LHCP2020** (2021) 242 [arXiv:2009.03877] [INSPIRE].

[12] A. Crivellin, F. Kirk, C.A. Manzari and M. Montull, *Global Electroweak Fit and Vector-Like Leptons in Light of the Cabibbo Angle Anomaly*, *JHEP* **12** (2020) 166 [arXiv:2008.01113] [INSPIRE].

[13] M. Kirk, *Cabibbo anomaly versus electroweak precision tests: An exploration of extensions of the Standard Model*, *Phys. Rev. D* **103** (2021) 035004 [arXiv:2008.03261] [INSPIRE].

[14] A. Crivellin and M. Hoferichter, *β Decays as Sensitive Probes of Lepton Flavor Universality*, *Phys. Rev. Lett.* **125** (2020) 111801 [arXiv:2002.07184] [INSPIRE].

[15] B. Capdevila, A. Crivellin, C.A. Manzari and M. Montull, *Explaining $b \to s\ell^+\ell^-$ and the Cabibbo angle anomaly with a vector triplet*, *Phys. Rev. D* **103** (2021) 015032 [arXiv:2005.13542] [INSPIRE].

[16] B. Belfatto and Z. Berezhiani, *Are the CKM anomalies induced by vector-like quarks? Limits from flavor changing and Standard Model precision tests*, *JHEP* **10** (2021) 079 [arXiv:2103.05549] [INSPIRE].

[17] A. Crivellin, M. Hoferichter and C.A. Manzari, *Fermi Constant from Muon Decay Versus Electroweak Fits and Cabibbo-Kobayashi-Maskawa Unitarity*, *Phys. Rev. Lett.* **127** (2021) 071801 [arXiv:2102.02825] [INSPIRE].

[18] D. Bryman, V. Cirigliano, A. Crivellin and G. Inguglia, *Testing Lepton Flavor Universality with Pion, Kaon, Tau, and Beta Decays*, *Ann. Rev. Nucl. Part. Sci.* **72** (2022) 69 [arXiv:2111.05338] [INSPIRE].

[19] V. Cirigliano, A. Crivellin, M. Hoferichter and M. Moulson, *Scrutinizing CKM unitarity with a new measurement of the $K_{\mu3}/K_{\mu2}$ branching fraction*, *Phys. Lett. B* **838** (2023) 137748 [arXiv:2208.11707] [INSPIRE].

[20] C.-Y. Seng, *First row CKM unitarity*, in the proceedings of the *20th Conference on Flavor Physics and CP Violation*, (2022) [arXiv:2207.10492] [INSPIRE].

[21] C.A. Manzari, *Explaining the Cabibbo Angle Anomaly*, *PoS* **EPS-HEP2021** (2022) 526 [arXiv:2111.04519] [INSPIRE].

[22] A. Crivellin, *Explaining the Cabibbo Angle Anomaly*, arXiv:2207.02507 [INSPIRE].

[23] O. Eberhardt et al., *Status of the fourth fermion generation before ICHEP2012: Higgs data and electroweak precision observables*, *Phys. Rev. D* **86** (2012) 074014 [arXiv:1207.0438] [INSPIRE].

[24] O. Eberhardt et al., *Impact of a Higgs boson at a mass of* 126 *GeV on the standard model with three and four fermion generations*, *Phys. Rev. Lett.* **109** (2012) 241802 [arXiv:1209.1101] [INSPIRE].

[25] J.A.L. Hewett and T.G. Rizzo, *Low-Energy Phenomenology of Superstring Inspired E_6 Models*, *Phys. Rept.* **183** (1989) 193 [INSPIRE].

[26] P. Langacker, *Grand Unified Theories and Proton Decay*, *Phys. Rept.* **72** (1981) 185 [INSPIRE].

[27] F. del Aguila and M.J. Bowick, *The Possibility of New Fermions With $\Delta I = 0$ Mass*, *Nucl. Phys. B* **224** (1983) 107 [INSPIRE].

[28] I. Antoniadis, *A Possible new dimension at a few TeV*, *Phys. Lett. B* **246** (1990) 377 [INSPIRE].

[29] N. Arkani-Hamed, S. Dimopoulos and J. March-Russell, *Stabilization of submillimeter dimensions: The New guise of the hierarchy problem*, *Phys. Rev. D* **63** (2001) 064020 [hep-th/9809124] [INSPIRE].

[30] N. Arkani-Hamed, A.G. Cohen, E. Katz and A.E. Nelson, *The Littlest Higgs*, *JHEP* **07** (2002) 034 [hep-ph/0206021] [INSPIRE].

[31] T. Han, H.E. Logan, B. McElrath and L.-T. Wang, *Phenomenology of the little Higgs model*, *Phys. Rev. D* **67** (2003) 095004 [hep-ph/0301040] [INSPIRE].

[32] W. Altmannshofer, S. Gori, M. Pospelov and I. Yavin, *Quark flavor transitions in $L_\mu - L_\tau$ models*, *Phys. Rev. D* **89** (2014) 095033 [arXiv:1403.1269] [INSPIRE].

[33] B. Gripaios, M. Nardecchia and S.A. Renner, *Linear flavour violation and anomalies in B physics*, *JHEP* **06** (2016) 083 [arXiv:1509.05020] [INSPIRE].

[34] P. Arnan, L. Hofer, F. Mescia and A. Crivellin, *Loop effects of heavy new scalars and fermions in $b \to s\mu^+\mu^-$*, *JHEP* **04** (2017) 043 [arXiv:1608.07832] [INSPIRE].

[35] P. Arnan, A. Crivellin, M. Fedele and F. Mescia, *Generic Loop Effects of New Scalars and Fermions in $b \to s\ell^+\ell^-$, $(g-2)_\mu$ and a Vector-like 4th Generation*, *JHEP* **06** (2019) 118 [arXiv:1904.05890] [INSPIRE].

[36] A. Crivellin, C.A. Manzari, M. Alguero and J. Matias, *Combined Explanation of the $Z \to b\bar{b}$ Forward-Backward Asymmetry, the Cabibbo Angle Anomaly, and $\tau \to \mu\nu\nu$ and $b \to s\ell^+\ell^-$ Data*, *Phys. Rev. Lett.* **127** (2021) 011801 [arXiv:2010.14504] [INSPIRE].

[37] C. Bobeth, A.J. Buras, A. Celis and M. Jung, *Patterns of Flavour Violation in Models with Vector-Like Quarks*, *JHEP* **04** (2017) 079 [arXiv:1609.04783] [INSPIRE].

[38] A. Czarnecki and W.J. Marciano, *The Muon anomalous magnetic moment: A Harbinger for 'new physics'*, *Phys. Rev. D* **64** (2001) 013014 [hep-ph/0102122] [INSPIRE].

[39] K. Kannike, M. Raidal, D.M. Straub and A. Strumia, *Anthropic solution to the magnetic muon anomaly: the charged see-saw*, *JHEP* **02** (2012) 106 [*Erratum ibid.* **10** (2012) 136] [arXiv:1111.2551] [INSPIRE].

[40] R. Dermisek and A. Raval, *Explanation of the Muon $g-2$ Anomaly with Vectorlike Leptons and its Implications for Higgs Decays*, *Phys. Rev. D* **88** (2013) 013017 [arXiv:1305.3522] [INSPIRE].

[41] A. Freitas, J. Lykken, S. Kell and S. Westhoff, *Testing the Muon $g-2$ Anomaly at the LHC*, *JHEP* **05** (2014) 145 [*Erratum ibid.* **09** (2014) 155] [arXiv:1402.7065] [INSPIRE].

[42] G. Bélanger, C. Delaunay and S. Westhoff, *A Dark Matter Relic From Muon Anomalies*, *Phys. Rev. D* **92** (2015) 055021 [arXiv:1507.06660] [INSPIRE].

[43] A. Aboubrahim, T. Ibrahim and P. Nath, *Leptonic g − 2 moments, CP phases and the Higgs boson mass constraint*, *Phys. Rev. D* **94** (2016) 015032 [arXiv:1606.08336] [INSPIRE].

[44] K. Kowalska and E.M. Sessolo, *Expectations for the muon g − 2 in simplified models with dark matter*, *JHEP* **09** (2017) 112 [arXiv:1707.00753] [INSPIRE].

[45] S. Raby and A. Trautner, *Vectorlike chiral fourth family to explain muon anomalies*, *Phys. Rev. D* **97** (2018) 095006 [arXiv:1712.09360] [INSPIRE].

[46] A. Choudhury et al., *Muon g − 2 and related phenomenology in constrained vector-like extensions of the MSSM*, *JHEP* **05** (2017) 072 [arXiv:1701.08778] [INSPIRE].

[47] L. Calibbi, R. Ziegler and J. Zupan, *Minimal models for dark matter and the muon g − 2 anomaly*, *JHEP* **07** (2018) 046 [arXiv:1804.00009] [INSPIRE].

[48] A. Crivellin, M. Hoferichter and P. Schmidt-Wellenburg, *Combined explanations of (g − 2)_{μ,e} and implications for a large muon EDM*, *Phys. Rev. D* **98** (2018) 113002 [arXiv:1807.11484] [INSPIRE].

[49] R. Capdevilla, D. Curtin, Y. Kahn and G. Krnjaic, *Discovering the physics of (g − 2)_μ at future muon colliders*, *Phys. Rev. D* **103** (2021) 075028 [arXiv:2006.16277] [INSPIRE].

[50] R. Capdevilla, D. Curtin, Y. Kahn and G. Krnjaic, *No-lose theorem for discovering the new physics of (g − 2)μ at muon colliders*, *Phys. Rev. D* **105** (2022) 015028 [arXiv:2101.10334] [INSPIRE].

[51] A. Crivellin and M. Hoferichter, *Consequences of chirally enhanced explanations of (g − 2)_μ for h → μμ and Z → μμ*, *JHEP* **07** (2021) 135 [*Erratum ibid.* **10** (2022) 030] [arXiv:2104.03202] [INSPIRE].

[52] L. Calibbi, X. Marcano and J. Roy, *Z lepton flavour violation as a probe for new physics at future e⁺e⁻ colliders*, *Eur. Phys. J. C* **81** (2021) 1054 [arXiv:2107.10273] [INSPIRE].

[53] G. Arcadi, L. Calibbi, M. Fedele and F. Mescia, *Systematic approach to B-physics anomalies and t-channel dark matter*, *Phys. Rev. D* **104** (2021) 115012 [arXiv:2103.09835] [INSPIRE].

[54] P. Paradisi, O. Sumensari and A. Valenti, *High-energy frontier of the muon g − 2 at a muon collider*, *Phys. Rev. D* **106** (2022) 115038 [arXiv:2203.06103] [INSPIRE].

[55] L. Allwicher et al., *What is the scale of new physics behind the muon g − 2?*, *Phys. Rev. D* **104** (2021) 055035 [arXiv:2105.13981] [INSPIRE].

[56] A. Crivellin, M. Kirk, T. Kitahara and F. Mescia, *Large t → cZ as a sign of vectorlike quarks in light of the W mass*, *Phys. Rev. D* **106** (2022) L031704 [arXiv:2204.05962] [INSPIRE].

[57] R. Balkin et al., *On the implications of positive W mass shift*, *JHEP* **05** (2022) 133 [arXiv:2204.05992] [INSPIRE].

[58] T.A. Chowdhury and S. Saad, *Leptoquark-vectorlike quark model for the CDF mW, (g − 2)μ, R_{K^{(∗)}} anomalies, and neutrino masses*, *Phys. Rev. D* **106** (2022) 055017 [arXiv:2205.03917] [INSPIRE].

[59] G.C. Branco and M.N. Rebelo, *Vector-like Quarks*, *PoS* **DISCRETE2020-2021** (2022) 004 [arXiv:2208.07235] [INSPIRE].

[60] G.C. Branco et al., *Addressing the CKM unitarity problem with a vector-like up quark*, *JHEP* **07** (2021) 099 [arXiv:2103.13409] [INSPIRE].

[61] S. Balaji, *Asymmetry in flavour changing electromagnetic transitions of vector-like quarks*, *JHEP* **05** (2022) 015 [arXiv:2110.05473] [INSPIRE].

[62] PIONEER collaboration, *Testing Lepton Flavor Universality and CKM Unitarity with Rare Pion Decays in the PIONEER experiment*, in the proceedings of the *Snowmass 2021*, (2022) [arXiv:2203.05505] [INSPIRE].

[63] J.C. Hardy and I.S. Towner, *Superallowed $0^+ \to 0^+$ nuclear β decays: 2020 critical survey, with implications for V_{ud} and CKM unitarity*, *Phys. Rev. C* **102** (2020) 045501 [INSPIRE].

[64] PARTICLE DATA GROUP collaboration, *Review of Particle Physics*, *PTEP* **2022** (2022) 083C01 [INSPIRE].

[65] L. Hayen, *Standard model $\mathcal{O}(\alpha)$ renormalization of g_A and its impact on new physics searches*, *Phys. Rev. D* **103** (2021) 113001 [arXiv:2010.07262] [INSPIRE].

[66] X. Feng et al., *First-principles calculation of electroweak box diagrams from lattice QCD*, *Phys. Rev. Lett.* **124** (2020) 192002 [arXiv:2003.09798] [INSPIRE].

[67] W.J. Marciano and A. Sirlin, *Improved calculation of electroweak radiative corrections and the value of V_{ud}*, *Phys. Rev. Lett.* **96** (2006) 032002 [hep-ph/0510099] [INSPIRE].

[68] UCNτ collaboration, *Improved neutron lifetime measurement with UCNτ*, *Phys. Rev. Lett.* **127** (2021) 162501 [arXiv:2106.10375] [INSPIRE].

[69] B. Märkisch et al., *Measurement of the Weak Axial-Vector Coupling Constant in the Decay of Free Neutrons Using a Pulsed Cold Neutron Beam*, *Phys. Rev. Lett.* **122** (2019) 242501 [arXiv:1812.04666] [INSPIRE].

[70] M. Gorchtein, *γW Box Inside Out: Nuclear Polarizabilities Distort the Beta Decay Spectrum*, *Phys. Rev. Lett.* **123** (2019) 042503 [arXiv:1812.04229] [INSPIRE].

[71] C.-Y. Seng and M. Gorchtein, *Dispersive formalism for the nuclear structure correction δ_{NS} to the β decay rate*, arXiv:2211.10214 [INSPIRE].

[72] FLAVOUR LATTICE AVERAGING GROUP (FLAG) collaboration, *FLAG Review 2021*, *Eur. Phys. J. C* **82** (2022) 869 [arXiv:2111.09849] [INSPIRE].

[73] M. Moulson, *Vus from Kaons*, in *CKM 2021*, (2021). https://indico.cern.ch/event/891123/contributions/4601856/.

[74] C.-Y. Seng, M. Gorchtein, H.H. Patel and M.J. Ramsey-Musolf, *Reduced Hadronic Uncertainty in the Determination of V_{ud}*, *Phys. Rev. Lett.* **121** (2018) 241804 [arXiv:1807.10197] [INSPIRE].

[75] C.Y. Seng, M. Gorchtein and M.J. Ramsey-Musolf, *Dispersive evaluation of the inner radiative correction in neutron and nuclear β decay*, *Phys. Rev. D* **100** (2019) 013001 [arXiv:1812.03352] [INSPIRE].

[76] A. Czarnecki, W.J. Marciano and A. Sirlin, *Radiative Corrections to Neutron and Nuclear Beta Decays Revisited*, *Phys. Rev. D* **100** (2019) 073008 [arXiv:1907.06737] [INSPIRE].

[77] K. Shiells, P.G. Blunden and W. Melnitchouk, *Electroweak axial structure functions and improved extraction of the Vud CKM matrix element*, *Phys. Rev. D* **104** (2021) 033003 [arXiv:2012.01580] [INSPIRE].

[78] C.-Y. Seng, D. Galviz, M. Gorchtein and U.-G. Meißner, *Improved K_{e3} radiative corrections sharpen the $K_{\mu2}$–K_{l3} discrepancy*, *JHEP* **11** (2021) 172 [arXiv:2103.04843] [INSPIRE].

[79] C.-Y. Seng, D. Galviz, M. Gorchtein and U.-G. Meißner, *Complete theory of radiative corrections to $K_{\ell3}$ decays and the V_{us} update*, *JHEP* **07** (2022) 071 [arXiv:2203.05217] [INSPIRE].

[80] M. Di Carlo et al., *Light-meson leptonic decay rates in lattice QCD+QED*, *Phys. Rev. D* **100** (2019) 034514 [arXiv:1904.08731] [INSPIRE].

[81] C.-Y. Seng, D. Galviz, M. Gorchtein and U.G. Meißner, *High-precision determination of the Ke3 radiative corrections*, *Phys. Lett. B* **820** (2021) 136522 [arXiv:2103.00975] [INSPIRE].

[82] C.-Y. Seng, D. Galviz, W.J. Marciano and U.-G. Meißner, *Update on $|V_{us}|$ and $|V_{us}/V_{ud}|$ from semileptonic kaon and pion decays*, *Phys. Rev. D* **105** (2022) 013005 [arXiv:2107.14708] [INSPIRE].

[83] KLOE-2 collaboration, *Measurement of the branching fraction for the decay $K_S \to \pi\mu\nu$ with the KLOE detector*, *Phys. Lett. B* **804** (2020) 135378 [arXiv:1912.05990] [INSPIRE].

[84] KLOE-2 collaboration, *Measurement of the $K_S \to \pi e\nu$ branching fraction with the KLOE experiment*, *JHEP* **02** (2023) 098 [arXiv:2208.04872] [INSPIRE].

[85] N. Carrasco et al., *$K \to \pi$ semileptonic form factors with $N_f = 2 + 1 + 1$ twisted mass fermions*, *Phys. Rev. D* **93** (2016) 114512 [arXiv:1602.04113] [INSPIRE].

[86] FERMILAB LATTICE and MILC collaborations, *$|V_{us}|$ from $K_{\ell3}$ decay and four-flavor lattice QCD*, *Phys. Rev. D* **99** (2019) 114509 [arXiv:1809.02827] [INSPIRE].

[87] N. Cabibbo, E.C. Swallow and R. Winston, *Semileptonic hyperon decays and CKM unitarity*, *Phys. Rev. Lett.* **92** (2004) 251803 [hep-ph/0307214] [INSPIRE].

[88] L.S. Geng, J. Martin Camalich and M.J. Vicente Vacas, *SU(3)-breaking corrections to the hyperon vector coupling $f_1(0)$ in covariant baryon chiral perturbation theory*, *Phys. Rev. D* **79** (2009) 094022 [arXiv:0903.4869] [INSPIRE].

[89] E. Gamiz et al., *$|V_{us}|$ and m_s from hadronic tau decays*, *Nucl. Phys. B Proc. Suppl.* **169** (2007) 85 [hep-ph/0612154] [INSPIRE].

[90] HFLAV collaboration, *Averages of b-hadron, c-hadron, and τ-lepton properties as of 2021*, *Phys. Rev. D* **107** (2023) 052008 [arXiv:2206.07501] [INSPIRE].

[91] A. Lusiani, *Prospects for $|V_{us}|$ determinations from tau decays*, in *Electroweak Precision Physics from Beta Decays to the Z Pole*, (2022) https://indico.mitp.uni-mainz.de/event/272/contributions/4119/.

[92] R.J. Hudspith, R. Lewis, K. Maltman and J. Zanotti, *A resolution of the inclusive flavor-breaking τ $|V_{us}|$ puzzle*, *Phys. Lett. B* **781** (2018) 206 [arXiv:1702.01767] [INSPIRE].

[93] K. Maltman et al., *Current Status of inclusive hadronic τ determinations of $|V_{us}|$*, *SciPost Phys. Proc.* **1** (2019) 006 [INSPIRE].

[94] A. Pich and J. Prades, *Strange quark mass determination from Cabibbo suppressed tau decays*, *JHEP* **10** (1999) 004 [hep-ph/9909244] [INSPIRE].

[95] RBC and UKQCD collaborations, *Continuum Limit Physics from 2+1 Flavor Domain Wall QCD*, *Phys. Rev. D* **83** (2011) 074508 [arXiv:1011.0892] [INSPIRE].

[96] RBC and UKQCD collaborations, *Novel $|V_{us}|$ Determination Using Inclusive Strange τ Decay and Lattice Hadronic Vacuum Polarization Functions*, *Phys. Rev. Lett.* **121** (2018) 202003 [arXiv:1803.07228] [INSPIRE].

[97] A. Lusiani, private communication.

[98] D. Giusti et al., *First lattice calculation of the QED corrections to leptonic decay rates*, *Phys. Rev. Lett.* **120** (2018) 072001 [arXiv:1711.06537] [INSPIRE].

[99] A. Lusiani, *Updated determinations of $|V_{us}|$ with tau decays using new recent estimates of radiative corrections for light-meson leptonic decay rates*, in the proceedings of the *16th International Workshop on Tau Lepton Physics* , (2022) [arXiv:2201.03272] [INSPIRE].

[100] M.A. Arroyo-Ureña et al., *Radiative corrections to $\tau \to \pi(K)\nu_\tau[\gamma]$: A reliable new physics test*, *Phys. Rev. D* **104** (2021) L091502 [`arXiv:2107.04603`] [InSPIRE].

[101] M.A. Arroyo-Ureña et al., *One-loop determination of $\tau \to \pi(K)\nu_\tau[\gamma]$ branching ratios and new physics tests*, *JHEP* **02** (2022) 173 [`arXiv:2112.01859`] [InSPIRE].

[102] A. Czarnecki, W.J. Marciano and A. Sirlin, *Pion beta decay and Cabibbo-Kobayashi-Maskawa unitarity*, *Phys. Rev. D* **101** (2020) 091301 [`arXiv:1911.04685`] [InSPIRE].

[103] CKMfitter Group collaboration, *CP violation and the CKM matrix: Assessing the impact of the asymmetric B factories*, *Eur. Phys. J. C* **41** (2005) 1 [`hep-ph/0406184`] [InSPIRE].

[104] UTfit collaboration, *New UTfit Analysis of the Unitarity Triangle in the Cabibbo-Kobayashi-Maskawa scheme*, `arXiv:2212.03894` [YITP-SB-2022-40] [InSPIRE].

[105] CHORUS collaboration, *Leading order analysis of neutrino induced dimuon events in the CHORUS experiment*, *Nucl. Phys. B* **798** (2008) 1 [`arXiv:0804.1869`] [InSPIRE].

[106] BESIII collaboration, *Precision measurements of $B(D^+ \to \mu^+\nu_\mu)$, the pseudoscalar decay constant f_{D^+}, and the quark mixing matrix element $|V_{cd}|$*, *Phys. Rev. D* **89** (2014) 051104 [`arXiv:1312.0374`] [InSPIRE].

[107] Belle-II collaboration, *The Belle II Physics Book*, *PTEP* **2019** (2019) 123C01 [*Erratum ibid.* **2020** (2020) 029201] [`arXiv:1808.10567`] [InSPIRE].

[108] BESIII collaboration, *Future Physics Programme of BESIII*, *Chin. Phys. C* **44** (2020) 040001 [`arXiv:1912.05983`] [InSPIRE].

[109] B. Grzadkowski, M. Iskrzynski, M. Misiak and J. Rosiek, *Dimension-Six Terms in the Standard Model Lagrangian*, *JHEP* **10** (2010) 085 [`arXiv:1008.4884`] [InSPIRE].

[110] CDF collaboration, *High-precision measurement of the W boson mass with the CDF II detector*, *Science* **376** (2022) 170 [InSPIRE].

[111] B. Belfatto and S. Trifinopoulos, *The remarkable role of the vector-like quark doublet in the Cabibbo angle and W-mass anomalies*, `arXiv:2302.14097` [InSPIRE].

[112] J. Aebischer, J. Kumar, P. Stangl and D.M. Straub, *A Global Likelihood for Precision Constraints and Flavour Anomalies*, *Eur. Phys. J. C* **79** (2019) 509 [`arXiv:1810.07698`] [InSPIRE].

[113] D. Straub, P. Stangl, M. Hudec and M. Kirk, *smelli/smelli: v2.3.2*, `DOI:10.5281/ZENODO.5544228`.

[114] D.M. Straub, *flavio: a Python package for flavour and precision phenomenology in the Standard Model and beyond*, `arXiv:1810.08132` [InSPIRE].

[115] J. Aebischer, J. Kumar and D.M. Straub, *Wilson: a Python package for the running and matching of Wilson coefficients above and below the electroweak scale*, *Eur. Phys. J. C* **78** (2018) 1026 [`arXiv:1804.05033`] [InSPIRE].

[116] J. Buchner et al., *X-ray spectral modelling of the AGN obscuring region in the CDFS: Bayesian model selection and catalogue*, *Astron. Astrophys.* **564** (2014) A125 [`arXiv:1402.0004`] [InSPIRE].

[117] F. Feroz, M.P. Hobson and M. Bridges, *MultiNest: an efficient and robust Bayesian inference tool for cosmology and particle physics*, *Mon. Not. Roy. Astron. Soc.* **398** (2009) 1601 [`arXiv:0809.3437`] [InSPIRE].

[118] F. Feroz, M.P. Hobson, E. Cameron and A.N. Pettitt, *Importance Nested Sampling and the MultiNest Algorithm*, *Open J. Astrophys.* **2** (2019) 10 [`arXiv:1306.2144`] [InSPIRE].

[119] D. Foreman-Mackey, *corner.py: Scatterplot matrices in Python*, *J. Open Source Softw.* **1** (2016) 24.

[120] S. Descotes-Genon et al., *The CKM parameters in the SMEFT*, *JHEP* **05** (2019) 172 [`arXiv:1812.08163`] [INSPIRE].

[121] J. Brod, S. Kvedaraite, Z. Polonsky and A. Youssef, *Electroweak corrections to the Charm-Top-Quark Contribution to ϵ_K*, *JHEP* **12** (2022) 014 [`arXiv:2207.07669`] [INSPIRE].

[122] M. Endo, T. Kitahara, S. Mishima and K. Yamamoto, *Revisiting Kaon Physics in General Z Scenario*, *Phys. Lett. B* **771** (2017) 37 [`arXiv:1612.08839`] [INSPIRE].

[123] C. Bobeth, A.J. Buras, A. Celis and M. Jung, *Yukawa enhancement of Z-mediated new physics in $\Delta S = 2$ and $\Delta B = 2$ processes*, *JHEP* **07** (2017) 124 [`arXiv:1703.04753`] [INSPIRE].

[124] M. Endo, T. Kitahara and D. Ueda, *SMEFT top-quark effects on $\Delta F = 2$ observables*, *JHEP* **07** (2019) 182 [`arXiv:1811.04961`] [INSPIRE].

[125] HFLAV collaboration, *CHARM21 Global Fit (allowing for CPV)*, https://hflav-eos.web.cern.ch/hflav-eos/charm/CHARM21/results_mix_cpv.html.

[126] A. Crivellin et al., *First-generation new physics in simplified models: from low-energy parity violation to the LHC*, *JHEP* **10** (2021) 221 [`arXiv:2107.13569`] [INSPIRE].

[127] QWEAK collaboration, *Precision measurement of the weak charge of the proton*, *Nature* **557** (2018) 207 [`arXiv:1905.08283`] [INSPIRE].

[128] M. Cadeddu et al., *Muon and electron g-2 and proton and cesium weak charges implications on dark Zd models*, *Phys. Rev. D* **104** (2021) 011701 [`arXiv:2104.03280`] [INSPIRE].

[129] C.S. Wood et al., *Measurement of parity nonconservation and an anapole moment in cesium*, *Science* **275** (1997) 1759 [`arXiv:5307.1759`] [INSPIRE].

[130] J. Guena, M. Lintz and M.A. Bouchiat, *Measurement of the parity violating 6S-7S transition amplitude in cesium achieved within 2×10^{-13} atomic-unit accuracy by stimulated-emission detection*, *Phys. Rev. A* **71** (2005) 042108 [`physics/0412017`] [INSPIRE].

[131] V. Bernard, M. Oertel, E. Passemar and J. Stern, *Tests of non-standard electroweak couplings of right-handed quarks*, *JHEP* **01** (2008) 015 [`arXiv:0707.4194`] [INSPIRE].

[132] ATLAS collaboration, *Search for heavy vector-like quarks coupling to light quarks in proton-proton collisions at $\sqrt{s} = 7\,TeV$ with the ATLAS detector*, *Phys. Lett. B* **712** (2012) 22 [`arXiv:1112.5755`] [INSPIRE].

[133] ATLAS collaboration, *Search for Single Production of Vector-like Quarks Coupling to Light Generations in $4.64\,fb^{-1}$ of Data at $\sqrt{s} = 7\,TeV$*, ATLAS-CONF-2012-137 (2012).

[134] ATLAS collaboration, *Search for pair production of a new heavy quark that decays into a W boson and a light quark in pp collisions at $\sqrt{s} = 8\,TeV$ with the ATLAS detector*, *Phys. Rev. D* **92** (2015) 112007 [`arXiv:1509.04261`] [INSPIRE].

[135] CMS collaboration, *Search for vectorlike light-flavor quark partners in proton-proton collisions at $\sqrt{s} = 8\,TeV$*, *Phys. Rev. D* **97** (2018) 072008 [`arXiv:1708.02510`] [INSPIRE].

[136] X.-M. Cui, Y.-Q. Li and Y.-B. Liu, *Search for pair production of the heavy vectorlike top partner in same-sign dilepton signature at the HL-LHC*, *Phys. Rev. D* **106** (2022) 115025 [`arXiv:2212.01514`] [INSPIRE].

[137] A. Carmona, A. Lazopoulos, P. Olgoso and J. Santiago, *Matchmakereft: automated tree-level and one-loop matching*, *SciPost Phys.* **12** (2022) 198 [`arXiv:2112.10787`] [INSPIRE].

[138] FlaviaNet Working Group on Kaon Decays collaboration, *An Evaluation of |V_us| and precise tests of the Standard Model from world data on leptonic and semileptonic kaon decays*, *Eur. Phys. J. C* **69** (2010) 399 [arXiv:1005.2323] [INSPIRE].

[139] V. Bernard, M. Oertel, E. Passemar and J. Stern, *Dispersive representation and shape of the K_{l3} form factors: Robustness*, *Phys. Rev. D* **80** (2009) 034034 [arXiv:0903.1654] [INSPIRE].

[140] M. Moulson, *Experimental determination of V_{us} from kaon decays*, in the proceedings of the *8th International Workshop on the CKM Unitarity Triangle*, (2014) [arXiv:1411.5252] [INSPIRE].

[141] O.P. Yushchenko et al., *High statistic study of the $K^- \to \pi^0 \mu^- \nu$ decay*, *Phys. Lett. B* **581** (2004) 31 [hep-ex/0312004] [INSPIRE].

[142] M. González-Alonso, O. Naviliat-Cuncic and N. Severijns, *New physics searches in nuclear and neutron β decay*, *Prog. Part. Nucl. Phys.* **104** (2019) 165 [arXiv:1803.08732] [INSPIRE].

[143] UCNA collaboration, *New result for the neutron β-asymmetry parameter A_0 from UCNA*, *Phys. Rev. C* **97** (2018) 035505 [arXiv:1712.00884] [INSPIRE].

[144] D. Mund et al., *Determination of the Weak Axial Vector Coupling from a Measurement of the Beta-Asymmetry Parameter A in Neutron Beta Decay*, *Phys. Rev. Lett.* **110** (2013) 172502 [arXiv:1204.0013] [INSPIRE].

[145] A. Kozela et al., *Measurement of transverse polarization of electrons emitted in free neutron decay*, *Phys. Rev. C* **85** (2012) 045501 [arXiv:1111.4695] [INSPIRE].

[146] Y.A. Mostovoi et al., *Experimental value of G_A/G_V from a measurement of both P-odd correlations in free-neutron decay*, *Phys. Atom. Nucl.* **64** (2001) 1955 [INSPIRE].

[147] G. Darius et al., *Measurement of the Electron-Antineutrino Angular Correlation in Neutron β Decay*, *Phys. Rev. Lett.* **119** (2017) 042502 [INSPIRE].

[148] N. Gubernari, A. Kokulu and D. van Dyk, *$B \to P$ and $B \to V$ Form Factors from B-Meson Light-Cone Sum Rules beyond Leading Twist*, *JHEP* **01** (2019) 150 [arXiv:1811.00983] [INSPIRE].

[149] CLEO collaboration, *Improved measurements of D meson semileptonic decays to pi and K mesons*, *Phys. Rev. D* **80** (2009) 032005 [arXiv:0906.2983] [INSPIRE].

[150] BESIII collaboration, *Study of Dynamics of $D^0 \to K^- e^+ \nu_e$ and $D^0 \to \pi^- e^+ \nu_e$ Decays*, *Phys. Rev. D* **92** (2015) 072012 [arXiv:1508.07560] [INSPIRE].

[151] BESIII collaboration, *Analysis of $D^+ \to \bar{K}^0 e^+ \nu_e$ and $D^+ \to \pi^0 e^+ \nu_e$ semileptonic decays*, *Phys. Rev. D* **96** (2017) 012002 [arXiv:1703.09084] [INSPIRE].

[152] NA62 collaboration, *Measurement of the very rare $K^+ \to \pi^+ \nu \bar{\nu}$ decay*, *JHEP* **06** (2021) 093 [arXiv:2103.15389] [INSPIRE].

[153] J. Brod, M. Gorbahn and E. Stamou, *Two-Loop Electroweak Corrections for the $K \to \pi \nu \bar{\nu}$ Decays*, *Phys. Rev. D* **83** (2011) 034030 [arXiv:1009.0947] [INSPIRE].

[154] A.J. Buras, M. Gorbahn, U. Haisch and U. Nierste, *Charm quark contribution to $K^+ \to \pi^+ \nu \bar{\nu}$ at next-to-next-to-leading order*, *JHEP* **11** (2006) 002 [*Erratum ibid.* **11** (2012) 167] [hep-ph/0603079] [INSPIRE].

[155] G. Buchalla and A.J. Buras, *The rare decays $K \to \pi \nu \bar{\nu}$, $B \to X \nu \bar{\nu}$ and $B \to l^+ l^-$: An Update*, *Nucl. Phys. B* **548** (1999) 309 [hep-ph/9901288] [INSPIRE].

[156] G. Isidori, F. Mescia and C. Smith, *Light-quark loops in $K \to \pi \nu \bar{\nu}$*, *Nucl. Phys. B* **718** (2005) 319 [hep-ph/0503107] [INSPIRE].

[157] F. Mescia and C. Smith, *Improved estimates of rare K decay matrix-elements from Kl3 decays*, *Phys. Rev. D* **76** (2007) 034017 [arXiv:0705.2025] [INSPIRE].

[158] KOTO collaboration, *Search for the $K_L \to \pi^0 \nu \bar{\nu}$ and $K_L \to \pi^0 X^0$ decays at the J-PARC KOTO experiment*, *Phys. Rev. Lett.* **122** (2019) 021802 [arXiv:1810.09655] [INSPIRE].

[159] C. Bobeth et al., *$B_{s,d} \to l^+l^-$ in the Standard Model with Reduced Theoretical Uncertainty*, *Phys. Rev. Lett.* **112** (2014) 101801 [arXiv:1311.0903] [INSPIRE].

[160] M. Gorbahn and U. Haisch, *Charm Quark Contribution to $K_L \to \mu^+\mu^-$ at Next-to-Next-to-Leading*, *Phys. Rev. Lett.* **97** (2006) 122002 [hep-ph/0605203] [INSPIRE].

[161] V. Chobanova et al., *Probing SUSY effects in $K_S^0 \to \mu^+\mu^-$*, *JHEP* **05** (2018) 024 [arXiv:1711.11030] [INSPIRE].

[162] LHCB collaboration, *Constraints on the $K_S^0 \to \mu^+\mu^-$ Branching Fraction*, *Phys. Rev. Lett.* **125** (2020) 231801 [arXiv:2001.10354] [INSPIRE].

[163] T. Blum et al., *The $K \to (\pi\pi)_{I=2}$ Decay Amplitude from Lattice QCD*, *Phys. Rev. Lett.* **108** (2012) 141601 [arXiv:1111.1699] [INSPIRE].

[164] J. Brod and M. Gorbahn, *Next-to-Next-to-Leading-Order Charm-Quark Contribution to the CP Violation Parameter ϵ_K and ΔM_K*, *Phys. Rev. Lett.* **108** (2012) 121801 [arXiv:1108.2036] [INSPIRE].

[165] J. Brod and M. Gorbahn, *ϵ_K at Next-to-Next-to-Leading Order: The Charm-Top-Quark Contribution*, *Phys. Rev. D* **82** (2010) 094026 [arXiv:1007.0684] [INSPIRE].

[166] ETM collaboration, *$\Delta S = 2$ and $\Delta C = 2$ bag parameters in the standard model and beyond from $N_f = 2 + 1 + 1$ twisted-mass lattice QCD*, *Phys. Rev. D* **92** (2015) 034516 [arXiv:1505.06639] [INSPIRE].

[167] P. Janot and S. Jadach, *Improved Bhabha cross section at LEP and the number of light neutrino species*, *Phys. Lett. B* **803** (2020) 135319 [arXiv:1912.02067] [INSPIRE].

[168] I. Brivio and M. Trott, *The Standard Model as an Effective Field Theory*, *Phys. Rept.* **793** (2019) 1 [arXiv:1706.08945] [INSPIRE].

[169] A. Freitas, *Higher-order electroweak corrections to the partial widths and branching ratios of the Z boson*, *JHEP* **04** (2014) 070 [arXiv:1401.2447] [INSPIRE].

[170] ALEPH et al. collaborations, *Precision electroweak measurements on the Z resonance*, *Phys. Rept.* **427** (2006) 257 [hep-ex/0509008] [INSPIRE].

[171] CDF and D0 collaborations, *Combination of CDF and D0 W-Boson Mass Measurements*, *Phys. Rev. D* **88** (2013) 052018 [arXiv:1307.7627] [INSPIRE].

[172] ATLAS collaboration, *Measurement of the W-boson mass in pp collisions at $\sqrt{s} = 7$ TeV with the ATLAS detector*, *Eur. Phys. J. C* **78** (2018) 110 [*Erratum ibid.* **78** (2018) 898] [arXiv:1701.07240] [INSPIRE].

[173] M. Awramik, M. Czakon, A. Freitas and G. Weiglein, *Precise prediction for the W boson mass in the standard model*, *Phys. Rev. D* **69** (2004) 053006 [hep-ph/0311148] [INSPIRE].

[174] M. Bjørn and M. Trott, *Interpreting W mass measurements in the SMEFT*, *Phys. Lett. B* **762** (2016) 426 [arXiv:1606.06502] [INSPIRE].

[175] ALEPH et al. collaborations, *Electroweak Measurements in Electron-Positron Collisions at W-Boson-Pair Energies at LEP*, *Phys. Rept.* **532** (2013) 119 [arXiv:1302.3415] [INSPIRE].

[176] LHCB collaboration, *Measurement of forward $W \to e\nu$ production in pp collisions at $\sqrt{s} = 8$ TeV*, *JHEP* **10** (2016) 030 [arXiv:1608.01484] [INSPIRE].

[177] D0 collaboration, *A measurement of the $W \to \tau\nu$ production cross section in $p\bar{p}$ collisions at* $\sqrt{s} = 1.8$ *TeV*, *Phys. Rev. Lett.* **84** (2000) 5710 [hep-ex/9912065] [INSPIRE].

[178] ATLAS collaboration, *Test of the universality of τ and μ lepton couplings in W-boson decays with the ATLAS detector*, *Nature Phys.* **17** (2021) 813 [arXiv:2007.14040] [INSPIRE].

[179] SLD collaboration, *First direct measurement of the parity violating coupling of the Z^0 to the s quark*, *Phys. Rev. Lett.* **85** (2000) 5059 [hep-ex/0006019] [INSPIRE].